Chapter 6

Flexible links

This chapter is devoted to modelling and control of robot manipulators with *flexible links*. This class of robots includes lightweight manipulators and/or large articulated structures that are encountered in a variety of conventional and nonconventional settings. From the point of view of applications, we can think about very long arms needed for accessing hostile environments (nuclear sites, underground waste deposits, deep sea, space, etc.) or automated crane devices for building construction. The ultimate challenge is the design of mechanical arms made of light materials that are suitable for typical industrial manipulation tasks, such as pick-and-place, assembly, or surface finishing. Lightweight structures are expected to improve performance of robots with typically low payload-to-arm weight ratio. As opposed to slow and bulky motion of conventional industrial manipulators, such robotic designs are expected to achieve fast and dexterous motion.

In order to fully exploit the potential offered by flexible robot manipulators, we must explicitly consider the effects of structural link flexibility and properly deal with active and/or passive control of vibrational behaviour. In this context, it is highly desirable to have an explicit, complete, and accurate *dynamic model* at disposal. The model should be explicit to provide a clear understanding of dynamic interaction and couplings, to be useful for control design, and to guide reduction or simplification of terms. The model should be complete in that, even if it is simple, it inherits the most relevant properties of the system. The model should be accurate as required for simulation purposes, design of advanced model-based nonlinear controllers, and off-line optimal trajectory planning. These general guidelines are even more important in the modelling of flexible robotic structures, where schemata or approximations of the modes of link deformation are unavoidably introduced. Symbolic manipulation packages may prove useful

to derive dynamic models in a systematic error-free way.

Once a dynamic model for a flexible manipulator is available, its validation goes through the experimental identification of the relevant parameters. Besides those parameters that are inherited from the rigid case (mass, inertia, etc.), we should also identify the set of structural resonant frequencies and of associated deformation profiles. In the following, we assume that the analytical model matches the experimental data up to the desired order of model accuracy.

On the other hand, the control problem for flexible robot manipulators belongs to the class of mechanical systems where the number of controlled variables is strictly less than the number of mechanical degrees of freedom; this complicates the control design, ruling out a number of solutions that work in the rigid case. Further, the linear effects of flexibility are not separated from the typical nonlinear effects of multibody rigid dynamics. Although an effective control system could take advantage of some partitioning of rigid and flexible dynamics, the analysis of its behaviour should face in general the overall nonlinearities; in this respect, the linear dynamics resulting in the case of a single-link arm is a remarkable exception.

In order to tackle problems of increasing difficulty, a convenient classification of control targets can be introduced. As a minimum requirement, we should be able to control *rapid positioning* of the flexible arm. This is not a trivial problem since it requires both the synthesis of optimal feedforward commands, i.e., limiting the excitement of flexibility, and the active suppression of residual vibrations. For a high-performance flexible manipulator, a more demanding task is that of *tracking* a smooth *trajectory* of motion. This can be assigned at the joint level, as if the manipulator were rigid; provided that link deformation is kept limited, satisfactory results may be obtained also at the end-effector level. Last, the most difficult problem is that of reproducing trajectories defined directly for the end effector of the flexible manipulator.

The material is organized in two parts, covering modelling issues and control problems and algorithms.

First, the dynamic modelling of a single flexible link is presented. This simple case is representative of the complexity induced by the distributed nature of flexibility, and thus it has been extensively investigated in the literature. On the usual assumptions of the Euler-Bernoulli beam, an *infinite-dimensional model* is derived which is exact for deflections in the range of linearity. The relevant properties of the zero/pole structure of this linear model are discussed and *finite-dimensional approximations* are introduced. Next, the basic steps for obtaining dynamic models for the general multilink case are illustrated, leading to fully nonlinear equations of motion. The energy-based Lagrange formulation is adopted as the most convenient

approach for describing the coupling of rigid and flexible body dynamics.

On the basis of the above models, a series of control strategies are investigated. For the problem of *point-to-point motion*, *linear controllers* provide satisfactory performance. A joint co-located PD control is shown to achieve asymptotic stabilization of any given manipulator configuration. We also discuss the use of linear control laws with feedback from the whole state, i.e., including deflection variables, for improved damping of vibration around the terminal position. The efficacy of *nonlinear control* methods is then emphasized for the accurate *tracking* of *joint trajectories* in multi-link flexible robot manipulators. In particular, we present the design of *inversion control* for input–output decoupling, and of *two-time scale control* based on a singularly perturbed model reformulation. Finally, the *end-effector trajectory tracking* problem is considered. Differently from the rigid manipulator and from the elastic joint case, the use of pure inversion strategies may lead here to closed-loop instabilities. The nature of this problem is analyzed in connection with the nonminimum phase characteristics of the system zero dynamics —a concept which has also a nonlinear counterpart. Two solutions are presented; namely, an inversion procedure defined in the *frequency domain*, suitable for the single link linear case, and a combined feedforward/feedback strategy based on *nonlinear regulation* theory.

6.1 Modelling of a single-link arm

The derivation of a linear dynamic model of a single-link flexible arm is presented below. Basic assumptions for the validity of the model are stated first, leading to the so-called Euler-Bernoulli beam equations of motion, in which terms of second or higher order in the deformation variables are neglected. The *modal analysis* is then accomplished as an eigenvalue problem for the resulting infinite-dimensional system; besides the exact *unconstrained* mode method, also the usual *constrained* mode approximation is considered. The possibility of obtaining a distributed parameter input–output transfer function is discussed. Finite-dimensional models are finally derived from a frequency-based truncation procedure. Some comments on other feasible approximations of link deformation using different sets of assumed modes conclude this section.

6.1.1 Euler-Bernoulli beam equations

Consider a robot arm with a single *flexible link* as in Fig. 6.1, moving on a horizontal plane. The arm is clamped at the base to a rigid hub that is driven in rotation by an ideal torque actuator, and has no tip payload. In

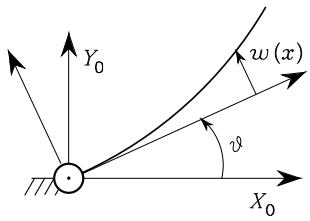

Figure 6.1: Schematic representation of single-link flexible arm.

order to derive a mathematical model, the following usual assumptions are made:

Assumption 6.1 The arm is a slender beam with uniform geometric characteristics and homogeneous mass distribution.

□

Assumption 6.2 The arm is flexible in the lateral direction, being stiff with respect to axial forces, torsion, and bending forces due to gravity; further, only elastic deformations are present.

□

Assumption 6.3 Nonlinear deformations as well as internal friction or other external disturbances are negligible effects.

□

Assumption 6.1 is the one that mainly characterizes *Euler-Bernoulli beam theory*, implying that the deflection of a section along the arm is due only to bending and not to shear. Moreover, the contribution of the rotary inertia of an arm section to the total energy is negligible. Notice that the analysis and the resulting partial differential equation will not represent those very high oscillation frequencies, whose wavelengths become comparable with the cross section of the arm. Assumption 6.2 is conveniently enforced by a suitable mechanical construction of the real flexible arm. Note that in Fig. 6.1 the small extension of the link along its neutral axis is neglected in the bending description; inclusion of this effect tends to stiffen the arm behaviour. Concerning Assumption 6.3, inclusion of nonlinear deformation terms is possible, while an accurate model of internal friction is usually difficult to obtain.

The system physical parameters of interest are: the linear density ρ, the flexural rigidity EI, the arm length ℓ, and the hub inertia I_h.

In order to derive the equations of motion for this system which is a combination of a lumped parameter part (the hub rotation) and of a distributed parameter part (the link deformation), an energy-based method is the most convenient, e.g., the Lagrange formulation or the Hamilton principle. Therefore, the kinetic energy T and the potential energy U of the system have to be computed.

For describing the arm kinematics, let t denote the time variable and x the space coordinate along the neutral axis of the beam; then, $\vartheta(t)$ is the angle of hub rotation and $w(x,t)$ is the beam deflection from the neutral axis. The absolute position vector of a point along the beam is then described by

$$p = \begin{pmatrix} p_x \\ p_y \end{pmatrix} = \begin{pmatrix} x\cos\vartheta(t) - w(x,t)\sin\vartheta(t) \\ x\sin\vartheta(t) + w(x,t)\cos\vartheta(t) \end{pmatrix}. \tag{6.1}$$

In the following, primes will denote differentiation with respect to x and dots differentiation with respect to t. Thus, $w'(x,t)$ is the angle of deflection of an arm section at distance x from the base. Moreover, since the beam is *clamped* at the base, we have the geometric boundary conditions

$$w(0,t) = w'(0,t) = 0. \tag{6.2}$$

The kinetic energy $T = T_h + T_\ell$ has contributions from the hub

$$T_h = \frac{1}{2} I_h \dot{\vartheta}(t)^2, \tag{6.3}$$

and from the link

$$\begin{aligned} T_\ell &= \frac{1}{2}\rho \int_0^\ell (\dot{p}_x^2 + \dot{p}_y^2) dx \qquad (6.4) \\ &= \frac{1}{2}\rho \int_0^\ell (x^2\dot{\vartheta}(t)^2 + y^2(x,t)\dot{\vartheta}(t)^2 + \dot{y}^2(x,t) + 2x\dot{\vartheta}(t)\dot{w}(x,t)) dx. \end{aligned}$$

The potential energy is

$$U = \frac{1}{2} EI \int_0^\ell (w''(x,t))^2 dx. \tag{6.5}$$

According to Hamilton principle, the system equations are obtained from the variational condition

$$\int_{t_1}^{t_2} (\delta T(t) - \delta U(t) + \delta W(t)) dt = 0, \tag{6.6}$$

where $\delta W(t) = u(t)\delta\vartheta(t)$ is the virtual work performed by the actuator driving torque $u(t)$. Grouping terms in (6.6) with respect to the independent variations $\delta\vartheta(t)$, $\delta w(x,t)$, $\delta w(\ell,t)$, and $\delta w'(\ell,t)$, and using calculus of variations arguments gives:

$$I_t\ddot{\vartheta}(t) + \rho\int_0^\ell x\ddot{w}(x,t)dx = u(t) \tag{6.7}$$

$$EIw''''(x,t) + \rho\ddot{w}(x,t) + \rho x\ddot{\vartheta}(t) = 0 \tag{6.8}$$

$$w(0,t) = w'(0,t) = 0 \tag{6.9}$$

$$w''(\ell,t) = w'''(\ell,t) = 0, \tag{6.10}$$

where $I_t = I_h + \rho\ell^3/3$. Eqs. (6.7) and (6.8) have been derived neglecting all second-order terms (products of state variables). The first equation can be attributed to the hub dynamics, while the second equation is associated with the flexible link. Note that, besides the geometric boundary conditions (6.9), the dynamic boundary conditions (6.10) arise at the tip representing balance of moment and of shearing force; in the absence of a payload, these are usually called *free* boundary conditions.

Integrating with respect to x eq. (6.8) multiplied by x and substituting in (6.7) yields

$$I_h\ddot{\vartheta}(t) - EIw''(0,t) = u(t) \tag{6.11}$$

that can be used in place of (6.7).

Eqs. (6.8)–(6.11) constitute the basis for the modal analysis of deformation in the Euler-Bernoulli beam. The distributed nature of the system is evidenced by the presence of partial differential equations.

6.1.2 Constrained and unconstrained modal analysis

As the system described by (6.8)–(6.11) is linear, we can proceed to compute eigenvalues and eigenvectors for the homogeneous system obtained by setting the forcing input $u(t) \equiv 0$. For the flexible arm, these will represent respectively the *resonant frequencies* and the associated *mode shapes*; this procedure is denoted in the literature as the *unconstrained mode* method. However, beam modal analysis is often performed by assuming also $\vartheta(t) \equiv 0$ (or $\ddot{\vartheta} = 0$), as if the rigid hub had infinite inertia and thus would be always at rest; this corresponds to the so-called *constrained mode* method.

We present first the constrained method because of its intrinsic simplicity. In this case, the link equation (6.8) becomes

$$w''''(x,t) + \frac{\rho}{EI}\ddot{w}(x,t) = 0 \tag{6.12}$$

with the same boundary conditions (6.9) and (6.10). This problem can be solved by separation of variables, setting

$$w(x,t) = \psi(x)\eta(t) \tag{6.13}$$

and substituting in (6.12). This gives in time and space

$$\ddot{\eta}(t) + \zeta^2\eta(t) = 0 \tag{6.14}$$

$$\psi''''(x) - \frac{\rho\zeta^2}{EI}\psi(x) = 0, \tag{6.15}$$

where ζ^2 is the eigenvalue and $\psi(x)$ is the *eigenfunction* of this *self-adjoint* boundary value problem. The general time solution to (6.14) is

$$\eta(t) = \eta(0)\cos(\zeta t) + \dot{\eta}(0)\sin(\zeta t), \tag{6.16}$$

representing an undamped harmonic oscillation at angular frequency ζ. From (6.9) and (6.10) the boundary conditions for $\psi(x)$ become

$$\psi(0) = \psi'(0) = 0 \tag{6.17}$$

$$\psi''(\ell) = \psi'''(\ell) = 0. \tag{6.18}$$

The general solution to (6.15) has the form

$$\psi(x) = A\sin(\beta x) + B\cos(\beta x) + C\sinh(\beta x) + D\cosh(\beta x) \tag{6.19}$$

for $x \in [0,\ell]$, where $\beta^4 = \rho\zeta^2/EI$, and the constants A, B, C, D are determined from (6.17) and (6.18) up to a scaling factor. From (6.17), it is $C = -A$ and $D = -B$. Then, in order to obtain a nontrivial solution for $\psi(x)$, the characteristic equation

$$1 + \cos(\beta\ell)\cosh(\beta\ell) = 0 \tag{6.20}$$

must hold, which follows from imposing (6.18). Accordingly, the solution takes on the form

$$\begin{aligned}\psi(x) = \psi_0\Big(&\big(\cos(\beta\ell) + \cosh(\beta\ell)\big)\big(\sinh(\beta x) - \sin(\beta x)\big)\\ &+\big(\sin(\beta\ell) + \sinh(\beta\ell)\big)\big(\cos(\beta x) - \cosh(\beta x)\big)\Big),\end{aligned} \tag{6.21}$$

where ψ_0 is a constant that is determined through a suitable normalization condition on the eigenfunction. Eq. (6.20) has a countable infinity of positive solutions $\{\beta_i,\ i = 1,2,\ldots\}$; an angular frequency $\zeta_i = \beta_i^2\sqrt{EI/\rho}$, a mode shape $\psi_i(x)$, and a time evolution $\eta_i(t)$ are obtained for each solution β_i.

The exact modal analysis is accomplished without forcing to zero $\ddot{\vartheta}(t)$. Hence, in the unconstrained mode method, we assume for $\vartheta(t)$ a solution of the form

$$\vartheta(t) = \alpha(t) + kv(t), \tag{6.22}$$

where $\alpha(t)$ describes the motion of the link center of mass, and for $w(x,t)$ a solution of the form

$$w(x,t) = \phi(x)v(t), \tag{6.23}$$

where k is chosen so as to satisfy

$$I_t k + \rho \int_0^\ell x\phi(x)dx = 0. \tag{6.24}$$

Note that eq. (6.24) guarantees that no perturbation of the motion of the center of mass occurs, i.e.,

$$\ddot{\alpha}(t) = 0. \tag{6.25}$$

Substituting (6.22) and (6.23) in (6.8) and taking into account (6.24) yields

$$\ddot{v}(t) + \omega^2 v(t) = 0 \tag{6.26}$$

$$\phi''''(x) - \frac{\rho\omega^2}{EI}(\phi(x) + kx) = 0, \tag{6.27}$$

where ω^2 is the eigenvalue and $\bar{\phi}(x) = \phi(x) + kx$ is the eigenfunction of the boundary value problem. The time solution to (6.26) is

$$v(t) = v(0)\cos(\omega t) + \dot{v}(0)\sin(\omega t). \tag{6.28}$$

The boundary conditions for $\phi(x)$ are

$$\phi(0) = \phi'(0) = 0 \tag{6.29}$$

$$\phi''(\ell) = \phi'''(\ell) = 0. \tag{6.30}$$

The general solution to (6.27) has the form

$$\phi(x) = A\sin(\gamma x) + B\cos(\gamma x) + C\sinh(\gamma x) + D\cosh(\gamma x) \tag{6.31}$$

for $x \in [0,\ell]$, where $\gamma^4 = \rho\omega^2/EI$, and the constants A, B, C, D are determined from (6.29) and (6.30) up to a scaling factor. It can be shown that the solution $\phi(x)$ has the form

$$\begin{aligned}\phi(x) = \phi_0\Big(&\big(\cos(\gamma\ell)\sinh(\gamma\ell) - \sin(\gamma\ell)\cosh(\gamma\ell)\big)\big(\cos(\gamma x) - \cosh(\gamma x)\big) \\ &+\big(1 + \sin(\gamma\ell)\sinh(\gamma\ell) + \cos(\gamma\ell)\cosh(\gamma\ell)\big)\big(\sin(\gamma x) - \sinh(\gamma x)\big) \\ &+2\big(1 + \cos(\gamma\ell)\cosh(\gamma\ell)\big)\big(\sinh(\gamma x) - \gamma x\big)\Big),\end{aligned} \tag{6.32}$$

where ϕ_0 is determined through a normalization condition, and γ has to satisfy the characteristic equation

$$I_h\gamma^3\big(1+\cos(\gamma\ell)\cosh(\gamma\ell)\big)+\rho\big(\sin(\gamma\ell)\cosh(\gamma\ell)-\cos(\gamma\ell)\sinh(\gamma\ell)\big)=0. \tag{6.33}$$

This equation derives from imposing a nontrivial solution to the linear homogeneous system obtained from (6.30) and (6.24). Notice that (6.33) has a double solution for $\gamma = 0$, accounting for the unconstrained (rigid body) motion at the link base. Also, when the hub inertia $I_h \to \infty$, this characteristic equation reduces to (6.20) with $\gamma \equiv \beta$ and the constrained model is fully recovered. This effect is enforced when closing a proportional control loop at the joint level with increasingly large gain.

As before, eq. (6.33) has a countable infinity of positive solutions $\{\gamma_i, i = 1, 2, \ldots\}$; an angular frequency $\omega_i = \gamma_i^2\sqrt{EI/\rho}$, a mode shape $\phi_i(x)$, a constant k_i, and a time evolution $v_i(t)$ (and then $\vartheta_i(t)$ from (6.22)) are obtained for each γ_i. In particular, from (6.11) and (6.24) it follows that

$$k_i = -\frac{EI}{I_h\omega_i^2}\phi_i''(0) = \bar{\phi}_i'(0). \tag{6.34}$$

From a system point of view, it is clear that the angular frequencies ω_i obtained with the above free evolution analysis will be the poles of the transfer function between the Laplace-transform $U(s)$ of the input and the Laplace-transform $Y(s)$ of any output taken for the flexible arm, e.g., hub rotation or tip position. It is worth noticing that distributed transfer functions can be derived, with no need to discretize a priori the system equations. In particular, taking the Laplace-transform of (6.11)

$$s^2 I_h\Theta(s) - EIW''(0,s) = U(s), \tag{6.35}$$

it can be shown that

$$W''(0,s) = -s^2\Theta(s)\frac{W_2(s)}{W_1(s)} \tag{6.36}$$

with

$$W_1(s) = \cos^2(\sigma\ell) + \cosh^2(\sigma\ell) \tag{6.37}$$

$$W_2(s) = \frac{\rho}{EI\sigma^3}\big(\sinh(\sigma\ell)\cosh(\sigma\ell) - \sin(\sigma\ell)\cos(\sigma\ell)\big), \tag{6.38}$$

and $2\sigma^2 = \sqrt{\rho/EI}s$. As a result, the transfer function from torque input to hub rotation output is

$$\frac{\Theta(s)}{U(s)} = \frac{W_1(s)}{s^2(I_hW_1(s) + EIW_2(s))}, \tag{6.39}$$

with the double pole at $s = 0$ accounting for the rigid body rotation. We point out the existence of a strict relation between the zeros of (6.39) and the characteristic solutions of the constrained modal analysis. In fact, from (6.37) the equation $W_1(s) = 0$ has no solution for $\sigma \in R$. On the other hand, by letting $\sigma = (\xi \pm j\xi)/2$ with $\xi \in R$, we find that $W_1(s) = 0$ when

$$1 + \cos(\xi\ell)\cosh(\xi\ell) = 0 \tag{6.40}$$

which coincides with (6.20). Then its positive roots are β_i, and the zeros of the transfer function are

$$s_i = 2\sqrt{\frac{EI}{\rho}}\sigma_i^2 = \pm j\sqrt{\frac{EI}{\rho}}\beta_i^2 \qquad i = 1, 2, \ldots \tag{6.41}$$

lying on the imaginary axis. The presence of some structural damping would move these zeros to the left complex half-plane. The location of zeros will be very important for the control problem, since high-gain output feedback as well as inversion control cause the open-loop zeros to become poles for the closed-loop system. In the above case of output taken at the joint level, the system is (marginally) *minimum-phase* and closed-loop stability is preserved.

6.1.3 Finite-dimensional models

From the previous development we can easily obtain *finite-dimensional* approximated models by including only a finite number of eigenvalues/eigenvectors. Considering the first n_e roots of (6.33), link deformation can be expressed in terms of n_e mode shapes as

$$w(x,t) = \sum_{i=1}^{n_e} \phi_i(x)v_i(t), \tag{6.42}$$

and accordingly

$$\vartheta(t) = \alpha(t) + \sum_{i=1}^{n_e} \phi_i'(0)v_i(t). \tag{6.43}$$

This allows transforming the nonhomogeneous equations (6.7)–(6.10) into a set of $n_e + 1$ second-order ordinary differential equations of the form:

$$I_t\ddot{\alpha}(t) = u(t) \tag{6.44}$$

$$\ddot{v}_i(t) + \omega_i^2 v_i(t) = \phi_i'(0)u(t) \qquad i = 1, \ldots, n_e \tag{6.45}$$

that can be rearranged in matrix form as

$$\begin{pmatrix} I_t & 0 \\ 0 & I \end{pmatrix} \begin{pmatrix} \ddot{\alpha} \\ \ddot{v} \end{pmatrix} + \begin{pmatrix} 0 & 0 \\ 0 & K \end{pmatrix} \begin{pmatrix} \alpha \\ v \end{pmatrix} = \begin{pmatrix} 1 \\ \phi'(0) \end{pmatrix} u, \tag{6.46}$$

where the zero blocks and the identity matrix I have proper dimensions. The decoupled nature of these equations is a consequence of the inherent orthogonality of the eigenfunctions $\phi_i(x)$. In particular, a diagonal $(n_e \times n_e)$ *stiffness matrix* $K = \text{diag}\{\omega_i^2\}$ is obtained. Link structural damping can be introduced in (6.46) either on the basis of the values in the stiffness matrix or observing experimentally the time decay of the system excited at each frequency of deformation; this leads to a term $D\dot{v}$ appearing in the lower equations of (6.46), with a diagonal $(n_e \times n_e)$ *damping matrix* D.

At this point, any similarity transformation can be performed on the vector $(\,\alpha \quad v^T\,)^T$ producing equivalent equations. For instance, in order to refer to a directly measurable quantity (the hub angle), eq. (6.46) can be represented as

$$\begin{pmatrix} I_t & -I_t\phi'(0)^T \\ -I_t\phi'(0) & I + I_t\phi'(0)\phi'(0)^T \end{pmatrix} \begin{pmatrix} \ddot{\vartheta} \\ \ddot{v} \end{pmatrix} + \begin{pmatrix} 0 & 0 \\ 0 & D \end{pmatrix} \begin{pmatrix} \dot{\vartheta} \\ \dot{v} \end{pmatrix} + \begin{pmatrix} 0 & 0 \\ 0 & K \end{pmatrix} \begin{pmatrix} \vartheta \\ v \end{pmatrix} = \begin{pmatrix} 1 \\ 0 \end{pmatrix} u \tag{6.47}$$

with a full inertia matrix, diagonal damping and stiffness terms, and the input torque appearing only in the first equation.

Standard $2(n_e + 1)$-dimensional state space representations can be immediately obtained from the above second-order dynamic models; for instance, by considering the hub rotation as system output and the state $x(t) = (\,\alpha \quad v^T \quad \dot{\alpha} \quad \dot{v}^T\,)^T$, the equations associated with (6.46) are of the form

$$\dot{x}(t) = Ax(t) + bu(t) \tag{6.48}$$

$$y(t) = c^T x(t) \tag{6.49}$$

with the triple (A, b, c^T) given by

$$A = \begin{pmatrix} 0 & 0 & 1 & 0 \\ 0 & 0 & 0 & I \\ -1/I_t & 0 & 0 & 0 \\ 0 & -K & 0 & -D \end{pmatrix} \qquad b = \begin{pmatrix} 0 \\ 0 \\ 1/I_t \\ \phi'(0) \end{pmatrix} \tag{6.50}$$

$$c^T = (\,1 \quad 0 \quad 0 \quad 0\,).$$

From (6.48), a finite-dimensional transfer function (i.e., with $n_e + 1$ poles and a finite number of zeros) replacing the distributed one is obtained as $Y(s)/U(s) = c^T(sI - A)^{-1}b$.

Other finite-dimensional models can be obtained by considering approximations other than simple truncation of the number of eigenfunctions. These are aimed at avoiding the complicated mode shape analysis involved by the exact (unconstrained) approach. A first example is represented by the constrained approximation in the above treated modal analysis; by assuming the finite expansion

$$w(x,t) = \sum_{i=1}^{n_e} \psi_i(x)\eta_i(t) \tag{6.51}$$

in place of (6.13) and proceeding as before, we get

$$\begin{pmatrix} I_t & \rho\mu^T \\ \rho\mu & \rho I \end{pmatrix} \begin{pmatrix} \ddot{\vartheta} \\ \ddot{\eta} \end{pmatrix} + \begin{pmatrix} 0 & 0 \\ 0 & \rho\hat{D} \end{pmatrix} \begin{pmatrix} \dot{\vartheta} \\ \dot{\eta} \end{pmatrix} + \begin{pmatrix} 0 & 0 \\ 0 & \rho\hat{K} \end{pmatrix} \begin{pmatrix} \vartheta \\ \eta \end{pmatrix} = \begin{pmatrix} 1 \\ 0 \end{pmatrix} u, \tag{6.52}$$

where $\hat{K} = \mathrm{diag}\{\zeta_i^2\}$, damping $\hat{D}$ was added similarly to (6.47), and

$$\mu = \left(\frac{\psi_1''(0)}{\beta_1^4} \quad \dots \quad \frac{\psi_{n_e}''(0)}{\beta_{n_e}^4} \right)^T. \tag{6.53}$$

Again, suitable orthogonality relations among the eigenfunctions $\psi_i(x)$ were used in (6.52). This approximate model, usually referred to as *clamped-free*, indeed displays a slightly different pattern of eigenvalues with respect to the exact one. However, the simplicity of the underlying computations needed to provide the coefficients in (6.52) makes the constrained approach quite appealing.

More in general, we can pursue simpler modelling techniques by assuming a finite number of mode shapes for the deformation, i.e.,

$$w(x,t) = \sum_{i=1}^{n_e} \varphi_i(x)\delta_i(t), \tag{6.54}$$

where the spatial *assumed modes* $\varphi_i(x)$ satisfy only a reduced set of boundary conditions, but no dynamic equations of motion like (6.8). When the assumed modes satisfy purely geometric boundary conditions, they are denoted as *admissible functions*; when the chosen deformation modes comply also with natural boundary conditions, they are called *comparison functions*. Incidentally, we remark that finite-element descriptions with concentrated elasticity as well as Ritz-Kantorovich expansions belong to the latter class of methods. The use of this type of assumed modes becomes necessary for treating more complex multilink flexible structures, far beyond the simple one-link arm considered in this section. On the other hand, nice features like dynamic orthogonality are lost and coupled equations typically result for the flexible motion.

6.2 Modelling of multilink manipulators

In order to obtain the dynamic model of a *multilink* robot manipulator, it is necessary to introduce a convenient kinematic description of the manipulator which takes into account the deformation of the links. For determining position and orientation of relevant link frames, a recursive procedure can be established similarly to the rigid case. Kinematic relationships are then used for computing kinetic and potential energy of the system within a Lagrange formulation. The modelling results of the previous section will be embedded in the description of each flexible link. In order to limit the complexity of the derivation, we will assume that rigid motion and link deformation occur in the same plane.

6.2.1 Direct kinematics

Consider a *planar* n-link flexible arm with revolute joints subject only to bending deformations without torsional effects; Fig. 6.2 shows a two-link example. The following coordinate frames are established: the inertial frame $(\hat{X}_0, \hat{Y}_0)$, the rigid body moving frame associated with link i (X_i, Y_i), and the flexible body moving frame associated with link i $(\hat{X}_i, \hat{Y}_i)$. The rigid motion is described by the joint angles ϑ_i, while $w_i(x_i)$ denotes the transversal deflection of link i at x_i with $0 \leq x_i \leq \ell_i$, being ℓ_i the link length.

Let ${}^i p_i(x_i) = (\, x_i \quad w_i(x_i)\,)^T$ be the position of a point along the deflected link i with respect to frame (X_i, Y_i) and p_i be the absolute position of the same point in frame $(\hat{X}_0, \hat{Y}_0)$. Also, ${}^i r_{i+1} = {}^i p_i(\ell_i)$ indicates the position of the origin of frame (X_{i+1}, Y_{i+1}) with respect to frame (X_i, Y_i), and r_{i+1} its absolute position in frame $(\hat{X}_0, \hat{Y}_0)$.

The joint (rigid) rotation matrix R_i and the rotation matrix E_i of the (flexible) link at the end point are, respectively,

$$R_i = \begin{pmatrix} \cos\vartheta_i & -\sin\vartheta_i \\ \sin\vartheta_i & \cos\vartheta_i \end{pmatrix} \qquad E_i = \begin{pmatrix} 1 & -w'_{ie} \\ w'_{ie} & 1 \end{pmatrix}, \tag{6.55}$$

where $w'_{ie} = (\partial w_i / \partial x_i)|_{x_i = \ell_i}$, and the linear approximation $\arctan w'_{ie} \simeq w'_{ie}$, valid for small deflections, has been made. This also implies that all second-order terms involving products of deformations will be neglected. Therefore, the above absolute position vectors can be expressed as

$$p_i = r_i + W_i {}^i p_i, \qquad r_{i+1} = r_i + W_i {}^i r_{i+1} \tag{6.56}$$

where W_i is the global transformation matrix from $(\hat{X}_0, \hat{Y}_0)$ to (X_i, Y_i), which obeys to the recursive equation

$$W_i = W_{i-1} E_{i-1} R_i = \hat{W}_{i-1} R_i \qquad \hat{W}_0 = I. \tag{6.57}$$

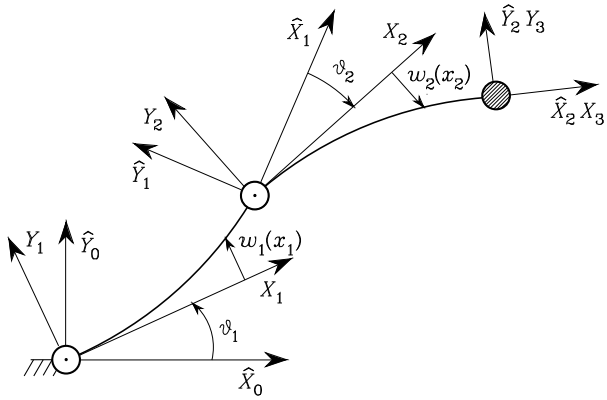

Figure 6.2: Schematic representation of a two-link flexible arm.

On the basis of the above relations, the kinematics of any point along the arm is fully characterized.

For later use in the arm kinetic energy, also the differential kinematics is needed. In particular, the (scalar) absolute angular velocity of frame (X_i, Y_i) is

$$\dot{\alpha}_i = \sum_{j=1}^{i} \dot{\vartheta}_j + \sum_{k=1}^{i-1} \dot{y}'_{ke}, \tag{6.58}$$

where the upper dot denotes time derivative. Moreover, the absolute linear velocity of an arm point is

$$\dot{p}_i = \dot{r}_i + \dot{W}_i {}^i p_i + W_i {}^i \dot{p}_i, \tag{6.59}$$

and ${}^i\dot{r}_{i+1} = {}^i\dot{p}_i(\ell_i)$. Since we neglect link axis extension ($\dot{x}_i = 0$), then ${}^i\dot{p}_i(x_i) = (\,0 \quad \dot{w}_i(x_i)\,)^T$. The computation of (6.59) takes advantage of the recursions

$$\dot{W}_i = \dot{\hat{W}}_{i-1} R_i + \hat{W}_{i-1} \dot{R}_i \qquad \dot{\hat{W}}_i = \dot{W}_i E_i + W_i \dot{E}_i. \tag{6.60}$$

Also, note that

$$\dot{R}_i = S R_i \dot{\vartheta}_i \qquad \dot{E}_i = S \dot{w}'_{ie} \qquad S = \begin{pmatrix} 0 & -1 \\ 1 & 0 \end{pmatrix}. \tag{6.61}$$

6.2.2 Lagrangian dynamics

The dynamic equations of motion of a planar n-link flexible arm can be derived following the standard *Lagrange formulation*, i.e., by computing the kinetic energy T and the potential energy U of the system and then forming the Lagrangian $L = T - U$.

The total *kinetic energy* is given by the sum of the following contributions:

$$T = \sum_{i=1}^{n} T_{hi} + \sum_{i=1}^{n} T_{\ell i} + T_p. \tag{6.62}$$

The kinetic energy of the rigid body located at hub i of mass m_{hi} and moment of inertia I_{hi} is

$$T_{hi} = \frac{1}{2} m_{hi} \dot{r}_i^T \dot{r}_i + \frac{1}{2} I_{hi} \dot{\alpha}_i^2 \tag{6.63}$$

with $\dot{\alpha}_i$ as in (6.58), the kinetic energy pertaining to the slender link i of linear density ρ_i is

$$T_{\ell i} = \frac{1}{2} \int_0^{\ell_i} \rho_i(x_i) \dot{p}_i(x_i)^T \dot{p}_i(x_i) dx_i, \tag{6.64}$$

and the kinetic energy associated with a payload of mass m_p and moment of inertia I_p located at the end of link n is

$$T_p = \frac{1}{2} m_p \dot{r}_{n+1}^T \dot{r}_{n+1} + \frac{1}{2} I_p (\dot{\alpha}_n + \dot{w}'_{ne})^2. \tag{6.65}$$

Remarkably, the evaluation of the expressions in (6.63) and (6.64) exploits the following identities:

$$R_i^T R_i = E_i^T E_i = S^T S = I \tag{6.66}$$

$$R_i^T \dot{R}_i = S \dot{\vartheta}_i \qquad E_i^T \dot{E}_i = \dot{w}'_{ie} (w'_{ie} I + S). \tag{6.67}$$

The *potential energy* is given by the sum of the following contributions:

$$U = \sum_{i=1}^{n} U_{ei} + \sum_{i=1}^{n} U_{ghi} + \sum_{i=1}^{n} U_{g\ell i} + U_{gp}. \tag{6.68}$$

The elastic energy stored in link i is

$$U_{ei} = \frac{1}{2} \int_0^{\ell_i} (EI)_i(x_i) \left(\frac{d^2 w_i(x_i)}{dx_i^2} \right)^2 dx_i, \tag{6.69}$$

being $(EI)_i$ its flexural rigidity. The gravitational energy of hub i is

$$U_{ghi} = -m_{hi} g_0^T r_i, \tag{6.70}$$

that of link i is

$$U_{g\ell i} = -g_0^T \int_0^{\ell_i} \rho_i(x_i) p_i(x_i) dx_i, \tag{6.71}$$

and that of the payload is

$$U_{gp} = -m_p g_0^T r_{n+1}, \tag{6.72}$$

being g_0 the gravity acceleration vector.

Notice that no discretization of structural link flexibility has been made so far. The Lagrangian L can be shown to generate an infinite-dimensional *nonlinear* model, which is of limited use for simulation and/or control purposes. Hence, in order to obtain a finite-dimensional dynamic model, the assumed modes link approximation (6.54) can be used. On the basis of this discretization, the Lagrangian L becomes a function of a set of $n + \sum_{i=1}^{n} n_{ei}$ generalized coordinates $\{\vartheta_i(t), \delta_{ij}(t)\}$, and the dynamic model is obtained by satisfying the Lagrange's equations

$$\frac{d}{dt}\frac{\partial L}{\partial \dot{\vartheta}_i} - \frac{\partial L}{\partial \vartheta_i} = u_i \qquad i = 1, \ldots, n \tag{6.73}$$

$$\frac{d}{dt}\frac{\partial L}{\partial \dot{\delta}_{ij}} - \frac{\partial L}{\partial \delta_{ij}} = 0 \qquad j = 1, \ldots, n_{ei},\ i = 1, \ldots, n, \tag{6.74}$$

where u_i is the joint torque at hub i. Note that no input torque appears on the right-hand side of the flexible equations, as can be inferred from the single-link equations (6.47) and (6.52). Thus, both unconstrained and constrained modes (or any other approximation) can be used in the model.

As a result, the equations of motion for a planar n-link flexible arm can be written in the closed form

$$\begin{pmatrix} H_{\vartheta\vartheta}(\vartheta,\delta) & H_{\vartheta\delta}(\vartheta,\delta) \\ H_{\vartheta\delta}^T(\vartheta,\delta) & H_{\delta\delta}(\vartheta,\delta) \end{pmatrix} \begin{pmatrix} \ddot{\vartheta} \\ \ddot{\delta} \end{pmatrix} + \begin{pmatrix} c_\vartheta(\vartheta,\delta,\dot{\vartheta},\dot{\delta}) \\ c_\delta(\vartheta,\delta,\dot{\vartheta},\dot{\delta}) \end{pmatrix} + \begin{pmatrix} g_\vartheta(\vartheta,\delta) \\ g_\delta(\vartheta,\delta) \end{pmatrix} + \begin{pmatrix} 0 \\ D\dot{\delta} + K\delta \end{pmatrix} = \begin{pmatrix} u \\ 0 \end{pmatrix}; \tag{6.75}$$

the positive definite symmetric inertia matrix H has been partitioned in blocks according to the rigid and flexible components, c is the vector of Coriolis and centrifugal forces, g is the vector of gravitational forces, while K and D are the system stiffness and damping diagonal matrices of proper

dimensions. We note that the linear expression $K\delta$ follows from rewriting the elastic energy U_e as —see also (6.69)—

$$U_e = \frac{1}{2}\delta^T K \delta. \tag{6.76}$$

By defining the configuration vector $q = (\vartheta^T \quad \delta^T)^T$, eqs. (6.75) can be compacted into

$$H(q)\ddot{q} + c(q,\dot{q}) + g(q) + \begin{pmatrix} 0 \\ D\dot{\delta} + K\delta \end{pmatrix} = \begin{pmatrix} u \\ 0 \end{pmatrix}. \tag{6.77}$$

As for the components of c, these can be evaluated as in the rigid case through the Christoffel symbols, i.e.,

$$c_i = \sum_j \sum_k \left(\frac{\partial H_{ij}}{\partial q_k} - \frac{1}{2}\frac{\partial H_{jk}}{\partial q_i} \right) \dot{q}_j \dot{q}_k. \tag{6.78}$$

6.2.3 Dynamic model properties

In the following, we list useful properties of the dynamic model (6.75).

Property 6.1 The spatial dependence present in the link kinetic and potential energy terms (6.64) and (6.71) can be resolved by the introduction of a number of constant parameters, characterizing the mechanical properties of the (uniform density) links:

$$\begin{aligned}
m_i &= \int_0^{\ell_i} \rho_i dx_i = \rho_i \ell_i \\
r_i &= \frac{1}{m_i}\int_0^{\ell_i} \rho_i x_i dx_i = \frac{1}{2}\ell_i \\
I_{oi} &= \int_0^{\ell_i} \rho_i x_i^2 dx_i = \frac{1}{3} m_i \ell_i^2 \\
\mu_{ij} &= \int_0^{\ell_i} \rho_i \varphi_{ij}(x_i) dx_i \\
\nu_{ij} &= \int_0^{\ell_i} \rho_i \varphi_{ij}(x_i) x_i dx_i \\
\varrho_{ijk} &= \int_0^{\ell_i} \rho_i \varphi_{ij}(x_i)\varphi_{ik}(x_i) dx_i \\
k_{ijk} &= \int_0^{\ell_i} (EI)_i \varphi''_{ij}(x_i)\varphi''_{ik}(x_i) dx_i.
\end{aligned} \tag{6.79}$$

Therefore, m_i is the mass of link i, r_i is the distance of center of mass of link i from joint i axis, I_{oi} is the inertia of link i about joint i axis, μ_{ij} and ν_{ij} are deformation moments of order zero and one of mode j of link i, and ϱ_{ijk} is the cross moment of modes j and k of link i. Also, k_{ijk} is the cross elasticity coefficient of modes j and k of link i (zero for $j \neq k$, when orthogonal modes are used). Although eq. (6.75) is in general highly nonlinear, it is not difficult to show that the left-hand side can be given a *linear* factorization of the type $Y(\vartheta, \delta, \dot{\vartheta}, \dot{\delta}, \ddot{\vartheta}, \ddot{\delta})a$, where the vector a contains all the above pre-computable parameters, while the regressor matrix Y has a known structure.

□

Property 6.2 A factorization of vector c in (6.77) exists

$$c(q, \dot{q}) = C(q, \dot{q})\dot{q} = \begin{pmatrix} C_{\vartheta\vartheta} & C_{\vartheta\delta} \\ C_{\delta\vartheta} & C_{\delta\delta} \end{pmatrix} \begin{pmatrix} \dot{\vartheta} \\ \dot{\delta} \end{pmatrix} \tag{6.80}$$

such that the matrix $N = \dot{H} - 2C$ is skew-symmetric. A possible choice is the one induced by (6.78). Moreover, a similar result holds for the block elements in (6.75); for instance, the matrix $N_{\delta\delta} = \dot{H}_{\delta\delta} - 2C_{\delta\delta}$ enjoys the same property.

□

Property 6.3 The choice of specific assumed modes implies convenient simplifications in the block $H_{\delta\delta}$ of the inertia matrix. In particular, orthonormality of the modes of each link induces a decoupled structure for the diagonal inertia subblocks of $H_{\delta\delta}$ which in turn may reduce to a constant diagonal one.

□

Property 6.4 A rather common approximation is to evaluate the total kinetic energy of the system in the undeformed configuration $\delta = 0$. This implies that the inertia matrix, and thus also c_ϑ and c_δ, are independent of δ. It can be shown that the velocity terms c_δ will then lose the quadratic dependence on $\dot{\delta}$. Moreover, if $H_{\delta\delta}$ is constant, c_ϑ too loses the quadratic dependence on $\dot{\delta}$, while each component of c_δ becomes a quadratic function of $\dot{\vartheta}$ only. Finally, if also $H_{\vartheta\delta}$, representing the coupling between the rigid body and the flexible body dynamics, is approximated by a constant matrix then $c_\delta \equiv 0$ and $c_\vartheta = C_{\vartheta\vartheta}(\vartheta, \dot{\vartheta})\dot{\vartheta}$, i.e., a quadratic function of $\dot{\vartheta}$ only.

□

Property 6.5 Due to the assumption of small deformation of each link, the dependence of the gravity term in the flexible equation is simply $g_\delta = g_\delta(\vartheta)$.

□

Property 6.6 It is expected that the flexible body dynamics is much faster than the rigid body dynamics, so that the dynamic model can be cast in a singularly perturbed form, similarly to the flexible joint case. Furthermore, if a clear frequency separation exists among the arm vibration modes, then the system can be effectively described on a multiple time-scale basis.

□

6.3 Regulation

We start the presentation of control laws for flexible arms by considering the classical *regulation* problem, i.e., the case of a *constant* desired equilibrium configuration $q_d = (\vartheta_d^T \quad \delta_d^T)^T$. Indeed, the arm deformation is zero for any value of the joint variables only in the absence of gravity. It is assumed that the full state of the flexible arm is available for feedback. However, when some structural damping is present, a linear feedback using only the joint variables will be shown to asymptotically stabilize the system. Otherwise, active vibration damping can be realized by designing a full state stabilizing control on the basis of the linear approximation of the arm dynamics around the terminal point. Although they are conceived for point-to-point tasks, the following schemes can also be applied in the terminal phase of a trajectory around the steady-state configuration.

6.3.1 Joint PD control

For the design of a *joint PD control* law, some considerations are in order concerning the terms in (6.75) deriving from the potential energy U.

In view of Assumption 6.2, we have that

$$U_e \leq U_{e\max} < \infty. \tag{6.81}$$

In view of (6.76), a direct consequence is that

$$\|\delta\| \leq \sqrt{\frac{2U_{e\max}}{\lambda_{\min}(K)}}. \tag{6.82}$$

Concerning the gravity contribution, the vector g satisfies the inequality

$$\left\| \frac{\partial g}{\partial q} \right\| \leq \alpha_0 + \alpha_1 \|\delta\| \leq \alpha_0 + \alpha_1 \sqrt{\frac{2U_{e\max}}{\lambda_{\min}(K)}} =: \alpha, \tag{6.83}$$

where $\alpha_0, \alpha_1, \alpha > 0$. This can be easily proved by observing that the gravity term contains only trigonometric functions of ϑ and linear/trigonometric

functions of δ, and using (6.82). As a direct consequence of (6.83), we have for any q_1, q_2:

$$\|g(q_1) - g(q_2)\| \leq \alpha \|q_1 - q_2\|. \tag{6.84}$$

Theorem 6.1 *Consider the control law*

$$u = K_P(\vartheta_d - \vartheta) - K_D\dot{\vartheta} + g_\vartheta(\vartheta_d, \delta_d), \tag{6.85}$$

where K_P and K_D are $(n \times n)$ symmetric positive definite matrices and δ_d is defined as

$$\delta_d = -K^{-1} g_\delta(\vartheta_d). \tag{6.86}$$

If

$$\lambda_{\min}(K_q) = \lambda_{\min} \begin{pmatrix} K_P & 0 \\ 0 & K \end{pmatrix} > \alpha, \tag{6.87}$$

with α as in (6.83), then

$$q = q_d \qquad \dot{q} = 0$$

is a globally asymptotically stable equilibrium point for the closed-loop system (6.75) and (6.85)

◇ ◇ ◇

Proof. The equilibrium points of the closed-loop system (6.75) and (6.85) satisfy the equations

$$g_\vartheta(\vartheta, \delta) = K_P(\vartheta_d - \vartheta) + g_\vartheta(\vartheta_d, \delta_d) \tag{6.88}$$

$$g_\delta(\vartheta) = -K\delta. \tag{6.89}$$

It is easy to recognize that (6.89) has a unique solution δ for any value of ϑ. Adding $K\delta_d + g_\delta(\vartheta_d) = 0$ to the right-hand side of (6.89) yields

$$\begin{aligned} K_q(q_d - q) &= \begin{pmatrix} K_P & 0 \\ 0 & K \end{pmatrix} \begin{pmatrix} \vartheta_d - \vartheta \\ \delta_d - \delta \end{pmatrix} \\ &= \begin{pmatrix} g_\vartheta(\vartheta, \delta) - g_\vartheta(\vartheta_d, \delta_d) \\ g_\delta(\vartheta) - g_\delta(\vartheta_d) \end{pmatrix} = g(q) - g(q_d). \end{aligned} \tag{6.90}$$

In view of (6.87), we have that, for $q \neq q_d$,

$$\|K_q(q_d - q)\| \geq K_{qm}\|q_d - q\| > \alpha\|q_d - q\| \geq \|g(q) - g(q_d)\|, \tag{6.91}$$

where the last inequality follows from (6.84). This implies that $\{q = q_d, \dot{q} = 0\}$ is the *unique* equilibrium point of the closed-loop system (6.75) and (6.85).

Consider the energy-based Lyapunov function candidate

$$V = \frac{1}{2}\dot{q}^T H \dot{q} + \frac{1}{2}(q_d - q)^T K_q (q_d - q) + U_g(q) - U_g(q_d) + (q_d - q)^T g(q_d) \geq 0, \tag{6.92}$$

where $U_g = \sum_{i=1}^{n}(U_{ghi} + U_{g\ell i}) + U_{gp}$ is the total gravitational energy. The function (6.92) vanishes only at the desired equilibrium point, due to (6.88)–(6.91). The time derivative of (6.92) along the trajectories of the closed-loop system (6.75) and (6.85) is

$$\begin{aligned}\dot{V} &= \dot{q}^T\left(H\ddot{q} + \frac{1}{2}\dot{H}\dot{q}\right) - \dot{q}^T K_q(q_d - q) + \dot{q}^T(g(q) - g(q_d)) \\ &= \dot{q}^T\left(\begin{pmatrix} K_P(\vartheta_d - \vartheta) - K_D\dot{\vartheta} + g_\vartheta(q_d) \\ -(D\dot{\delta} + K\delta) \end{pmatrix} - g(q)\right) \\ &\quad -\dot{q}^T\begin{pmatrix} K_P(\vartheta_d - \vartheta) \\ K(\delta_d - \delta) \end{pmatrix} + \dot{q}^T\left(g(q) - \begin{pmatrix} g_\vartheta(q_d) \\ g_\delta(\vartheta_d) \end{pmatrix}\right),\end{aligned} \tag{6.93}$$

where identity (6.80) and the skew-symmetry of the matrix N have been used. Simplifying terms yields

$$\dot{V} = -\dot{\vartheta}^T K_D \dot{\vartheta} - \dot{\delta}^T D \dot{\delta} \leq 0, \tag{6.94}$$

where (6.86) has been utilized. When $\dot{V} = 0$, it is $\dot{q} = 0$ and the closed-loop system (6.75) and (6.85) becomes

$$H\ddot{q} = \begin{pmatrix} K_P(\vartheta_d - \vartheta) + g_\vartheta(q_d) - g_\vartheta(q) \\ -(K\delta + g_\delta(\vartheta)) \end{pmatrix}. \tag{6.95}$$

In view of the previous equilibrium analysis and of (6.87), it is $\ddot{q} = 0$ if and only if $q = q_d$, or $\vartheta = \vartheta_d$ and $\delta = \delta_d$. Invoking La Salle's invariant set theorem, global asymptotic stability of the desired point follows.

◇

Remarks

- The above control law does not require any feedback from the deflection variables, and is composed of a *linear* term plus a *constant feedforward* action which includes only part of the gravity force appearing in the model (6.75). The satisfaction of the structural assumption $\lambda_{\min}(K) > \alpha$ is not restrictive in general, and depends on the relative importance of stiffness vs. gravity.

- Condition (6.87) will automatically be satisfied, provided that the assumption on the structural link flexibility

$$\lambda_{\min}(K) > \alpha \tag{6.96}$$

holds, and that the proportional control gain is chosen so that the condition

$$\lambda_{\min}(K_p) > \alpha \tag{6.97}$$

is verified.

- The knowledge of the link stiffness K and of the complete gravity term g is needed in the definition of the steady-state deformation δ_d. Uncertainty in the associated model parameters produces a different asymptotically stable equilibrium point, which can be made arbitrarily close to the desired one by increasing K_P.

- It can be shown that stability is guaranteed even in the absence of link internal damping ($D = 0$). Physically, some small damping will always exist but the regulation transients could be very slow. If desired, a passive increase of damping can be achieved by structural modification, e.g., viscoelastic layer damping treatment.

- If the tip location is of interest, $p = k(\vartheta, \delta)$, then ϑ_d can be computed by inverting for ϑ the direct kinematics equation

$$k(\vartheta, -K^{-1} g_\delta(\vartheta)) = p_d, \tag{6.98}$$

so as to achieve end-effector regulation at steady-state.

6.3.2 Vibration damping control

During the execution of a point-to-point task, the arm typically undergoes dynamic deformations which are excited by the imposed accelerations. At the terminal point, the residual arm deformation is expected to vanish in accordance with the damping characteristics of the mechanical structure. These can be enhanced by the choice of suitable materials and surface treatment of the links. When passive damping is too low, oscillations will persist in the flexible arm long after the completion of the useful motion. To overcome this drawback, we need to have measurements related to arm deflection and use them properly in a feedback stabilizing control. *Active vibration linear control* can be designed as follows.

The first step is to linearize the nonlinear system dynamics (6.75) around the given (final) arm configuration q_d. Since at the equilibrium (6.86) holds,

setting $\Delta q = q_d - q$, $\Delta u = u_d - u$ with $u_d = g_\vartheta(q_d)$, and neglecting second and higher-order terms yields

$$\begin{pmatrix} H_{\vartheta\vartheta}(q_d) & H_{\vartheta\delta}(q_d) \\ H^T_{\vartheta\delta}(q_d) & H_{\delta\delta}(q_d) \end{pmatrix} \begin{pmatrix} \Delta\ddot{\vartheta} \\ \Delta\ddot{\delta} \end{pmatrix} + \begin{pmatrix} 0 & 0 \\ 0 & D \end{pmatrix} \begin{pmatrix} \Delta\dot{\vartheta} \\ \Delta\dot{\delta} \end{pmatrix} + \begin{pmatrix} \dfrac{\partial g_\vartheta}{\partial\vartheta}(q_d) & \dfrac{\partial g_\vartheta}{\partial\delta}(q_d) \\ \dfrac{\partial g_\delta}{\partial\vartheta}(q_d) & K \end{pmatrix} \begin{pmatrix} \Delta\vartheta \\ \Delta\delta \end{pmatrix} = \begin{pmatrix} \Delta u \\ 0 \end{pmatrix}. \tag{6.99}$$

A suitable state space representation of (6.99) is obtained by choosing

$$\Delta x = \begin{pmatrix} \Delta q \\ H(q_d)\Delta\dot{q} \end{pmatrix}, \tag{6.100}$$

i.e., variations of positions and of generalized momenta. By defining

$$M = \begin{pmatrix} M_{\vartheta\vartheta} & M_{\vartheta\delta} \\ M^T_{\vartheta\delta} & M_{\delta\delta} \end{pmatrix} = H^{-1}(q_d), \tag{6.101}$$

the linear state equations become

$$\begin{aligned} \Delta\dot{x} &= \begin{pmatrix} 0 & 0 & M_{\vartheta\vartheta} & M_{\vartheta\delta} \\ 0 & 0 & M^T_{\vartheta\delta} & M_{\delta\delta} \\ -\dfrac{\partial g_\vartheta}{\partial\vartheta} & -\dfrac{\partial g_\vartheta}{\partial\delta} & 0 & 0 \\ -\dfrac{\partial g_\delta}{\partial\vartheta} & -K & -DM^T_{\vartheta\delta} & -DM_{\delta\delta} \end{pmatrix} \Delta x + \begin{pmatrix} 0 \\ 0 \\ I \\ 0 \end{pmatrix} \Delta u \\ &= A\Delta x + B\Delta u. \end{aligned} \tag{6.102}$$

The linear stabilizing full state feedback can be designed as

$$\Delta u = F\Delta x = K_P\Delta\vartheta + K_D\Delta\dot{\vartheta} + K_{P\delta}\Delta\delta + K_{D\delta}\Delta\dot{\delta} \tag{6.103}$$

according to well-established methods, e.g., a pole placement technique. In order to assign any desired set of stable poles, it is necessary and sufficient that the pair (A, B) be controllable; it is not difficult to check that this condition always holds.

A convenient choice is to have the feedback matrix gains in (6.103) in block-diagonal form, corresponding to a decentralized strategy in which each stabilizing input component Δu_i uses only local information from link i; this can be achieved typically under more restrictive controllability conditions. Moreover, a pure damping action can be performed on the

deformation modes by setting $K_{P\delta} = 0$; in this way, uncertainty in the knowledge of the static deflection δ_d due to gravity —see (6.86)— turns only into a mismatch in the constant feedforward component u_d, while the system is still asymptotically stabilized around a different (perturbed) configuration.

We remark that the whole procedure can be applied also by linearizing the dynamics along a nominal trajectory, which gives a linear time-varying system whose stabilization by constant feedback is much more critical, though.

6.4 Joint tracking control

When trajectory tracking is of concern, performance of the above class of linear controllers is usually quite poor. It is then necessary to resort to *nonlinear control* strategies that take into account the largely varying dynamic couplings of the flexible robot arm during motion. The goal is to reproduce a time-varying smooth reference trajectory $q_d(t) = (\,\vartheta_d^T(t) \quad \delta_d^T(t)\,)^T$ characterizing the desired behaviour. However, due to the fact that fewer control inputs than configuration variables are available, it is in general not possible to achieve simultaneous tracking of both joint and deflection variables, unless the latter are defined in a consistent manner with the former. Upon this premise, an input–output *inversion* controller will be presented that guarantees exact reproduction of a desired joint trajectory $\vartheta_d(t)$, while inducing a bounded evolution for $\delta(t)$. An alternative design will be introduced that exploits the typical *two-time scale* nature of the rigid plus flexible equations of motion, providing approximate reproduction of $\vartheta_d(t)$. Both these model-based nonlinear control laws ensure closed-loop stability without any additional action required.

6.4.1 Inversion control

Trajectory tracking in nonlinear systems is typically achieved by input–output *inversion control* techniques. Once a meaningful output has been defined for the system, a nonlinear state feedback is designed so that the resulting closed-loop system is transformed into a linear and decoupled one, with the possible appearance of an unobservable internal dynamics. On the assumption of stability of the resulting closed-loop system, *exact* reproduction of smooth desired output trajectories is feasible.

For the purpose of control derivation, it is convenient to extract the

flexible accelerations from (6.75) as

$$\ddot{\delta} = -H_{\delta\delta}^{-1}\left(c_\delta + g_\delta + D\dot{\delta} + K\delta + H_{\vartheta\delta}^T\ddot{\vartheta}\right) \tag{6.104}$$

which, substituted into the upper part of (6.75), gives

$$(H_{\vartheta\vartheta} - H_{\vartheta\delta}H_{\delta\delta}^{-1}H_{\vartheta\delta}^T)\ddot{\vartheta} + c_\vartheta + g_\vartheta - H_{\vartheta\delta}H_{\delta\delta}^{-1}(c_\delta + g_\delta + D\dot{\delta} + K\delta) = u. \tag{6.105}$$

Notice that eq. (6.105) describes the modification that undergoes the rigid body dynamics due to the effects of link flexibility. The matrix $H_{\vartheta\vartheta} - H_{\vartheta\delta}H_{\delta\delta}^{-1}H_{\vartheta\delta}^T$ has full rank as can be seen from the following identity

$$\begin{pmatrix} H_{\vartheta\vartheta} & H_{\vartheta\delta} \\ H_{\vartheta\delta}^T & H_{\delta\delta} \end{pmatrix}\begin{pmatrix} I & 0 \\ -H_{\delta\delta}^{-1}H_{\vartheta\delta}^T & I \end{pmatrix} = \begin{pmatrix} H_{\vartheta\vartheta} - H_{\vartheta\delta}H_{\delta\delta}^{-1}H_{\vartheta\delta}^T & H_{\vartheta\delta} \\ 0 & H_{\delta\delta} \end{pmatrix} \tag{6.106}$$

and the positive definiteness of the inertia matrix.

We define the system output as the vector of joint variables ϑ. Following the inversion algorithm, this output needs to be differentiated as many times as until the input explicitly appearing. Inspection of eq. (6.105) suggests that the joint accelerations $\ddot{\vartheta}$ are at the same differential level as the torque inputs u. Therefore, the *relative degree* is uniform for all outputs and equal to *two*, and the input u can be fully recovered from (6.105).

Let u_0 denote a joint acceleration vector. Setting $\ddot{\vartheta} = u_0$ in (6.105) and solving for u yields the feedback law

$$u = (H_{\vartheta\vartheta} - H_{\vartheta\delta}H_{\delta\delta}^{-1}H_{\vartheta\delta}^T)u_0 + c_\vartheta + g_\vartheta - H_{\vartheta\delta}H_{\delta\delta}^{-1}(c_\delta + g_\delta + D\dot{\delta}) + K\delta, \tag{6.107}$$

where $(H_{\vartheta\vartheta} - H_{\vartheta\delta}H_{\delta\delta}^{-1}H_{\vartheta\delta}^T)^{-1}$ is the so-called *decoupling matrix* of the system and is nonsingular. From (6.107) it can be recognized that only the inversion of the block relative to the flexible variables is required for control law implementation. Hence, the complexity of this nonlinear feedback strategy increases only with the number of flexible variables; in the limit, no inertia matrix inversion is required for the rigid case and the inversion control law reduces to the well-known *inverse dynamics control*. Further, if $H_{\delta\delta}$ is constant, its inversion can be conveniently performed once for all off-line.

The control (6.107) transforms the closed-loop system (6.105) into the input–output linearized form

$$\ddot{\vartheta} = u_0 \tag{6.108}$$

$$\ddot{\delta} = -H_{\delta\delta}^{-1}(H_{\vartheta\delta}^T u_0 + c_\delta + g_\delta + D\dot{\delta} + K\delta). \tag{6.109}$$

In order to achieve tracking of a desired trajectory $\vartheta_d(t)$, the control design is completed by choosing the joint acceleration as

$$u_0 = \ddot{\vartheta}_d + K_D(\dot{\vartheta}_d - \dot{\vartheta}) + K_P(\vartheta_d - \vartheta), \tag{6.110}$$

where $K_P > 0$, $K_D > 0$ are feedback matrix gains that allow pole placement in the open left-hand complex half plane for the linear input–output part (6.108). From (6.110) it is clear that the desired trajectory must be differentiable at least once for having exact reproduction.

As previously mentioned, the applicability of the inversion controller (6.107) is based on the stability of the induced unobservable dynamics (6.109). The analysis can be carried out by studying the so-called *zero dynamics* associated with the system (6.108) and (6.109). This dynamics is obtained by constraining the output ϑ of the system to be a constant, without loss of generality zero. Hence, from (6.109) we obtain

$$\ddot{\delta} = -H_{\delta\delta}^{-1}(c_\delta + g_\delta + D\dot{\delta} + K\delta), \tag{6.111}$$

where functional dependence is dropped but it is intended that terms are evaluated for $\dot{\vartheta} = 0$.

A sufficient condition that guarantees at least local stability of the overall closed-loop system is that the zero dynamics (6.111) is *asymptotically stable*.

Lemma 6.1 *The state*

$$\delta = \delta_d = -K^{-1}g_\delta(\vartheta_d) \qquad \dot{\delta} = 0$$

is a globally asymptotically stable equilibrium point for system (6.111).

◇ ◇ ◇

Proof. The proof goes through a similar Lyapunov direct method argument as in Section 6.3.1, using the energy-based candidate function — see (6.92)—

$$\begin{aligned} V = &\frac{1}{2}\dot{\delta}^T B_{\delta\delta}\dot{\delta} + \frac{1}{2}(\delta_d - \delta)^T K(\delta_d - \delta) \\ &+U_g(\vartheta_d, \delta) - U_g(\vartheta_d, \delta_d) + (\delta_d - \delta)^T g_\delta(\vartheta_d), \end{aligned} \tag{6.112}$$

and exploiting the skew-symmetry of $N_{\delta\delta} = \dot{H}_{\delta\delta} - 2C_{\delta\delta}$.

◇

This lemma ensures also the overall closed-loop stability of system (6.108)–(6.110) when the regulation case is considered.

The above result is useful also in the trajectory tracking case ($\dot{\vartheta}_d \neq 0$). For instance, consider the simpler case of an inertia matrix independent of δ. When $\vartheta = \vartheta_d(t)$ is imposed by the inversion control, from (6.109) the flexible variables satisfy the following *linear time-varying* equation

$$\ddot{\delta} = f_\delta(t) - A_2(t)\dot{\delta} - A_1(t)\delta, \tag{6.113}$$

where

$$f_\delta(t) = -H_{\delta\delta}^{-1}(\vartheta_d)\big(H_{\vartheta\delta}^T(\vartheta_d)\ddot{\vartheta}_d + c_\delta(\vartheta_d, \dot{\vartheta}_d) + g_\delta(\vartheta_d)\big) \tag{6.114}$$

is a known function of time, and

$$A_1(t) = -H_{\delta\delta}^{-1}(\vartheta_d)K, \tag{6.115}$$

$$A_2(t) = -H_{\delta\delta}^{-1}(\vartheta_d)D. \tag{6.116}$$

Then, as long as all time-varying functions are bounded, stability is ensured by Lemma 6.1 even during trajectory tracking. However, in general, we have to check a further condition; namely, the input-to-state stability of the closed-loop system.

In the above derivation of the inversion control, it was assumed that full state feedback is available, i.e., ϑ, $\dot{\vartheta}$, δ, $\dot{\delta}$ should be measurable. In general, joint positions and velocities are measured via ordinary encoders and tachometers mounted on the actuators, while for link deflection different apparatus can be used ranging from strain gauges to accelerometers or optical devices. Nevertheless, in spite of the availability of direct measurements of link flexibility, it may be convenient to avoid their use within the computation of the nonlinear part of the controller. The joint-based approach lends itself to a cheap implementation in terms of joint variable measures only, obtained by keeping the robustifying linear feedback (6.110) and performing the nonlinear compensation as a *feedforward* action. This generalizes in a natural way the linear PD control (6.85) to the tracking case.

Specifically, given a differentiable joint trajectory $\vartheta_d(t)$, forward integration of the flexible dynamics

$$\ddot{\delta} = -H_{\delta\delta}^{-1}(\vartheta_d, \delta)\big(c_\delta(\vartheta_d, \delta, \dot{\vartheta}_d, \dot{\delta}) + g_\delta(\vartheta_d) + D\dot{\delta} + K\delta + H_{\vartheta\delta}^T(\vartheta_d, \delta)\ddot{\vartheta}_d\big) \tag{6.117}$$

from initial conditions $\delta(0) = \delta_0$, $\dot{\delta}(0) = \dot{\delta}_0$ provides the nominal evolutions $\delta_d(t)$, $\dot{\delta}_d(t)$ of the flexible variables. Hence, evaluation of the nonlinearities in (6.107) along the computed state trajectory gives a control law in the form

$$u = u_d(t) + K_P(t)(\vartheta_d - \vartheta) + K_D(t)(\dot{\vartheta}_d - \dot{\vartheta}), \tag{6.118}$$

where (6.110) has been used, and

$$\begin{aligned} u_d(t) = {} & H_{\vartheta\vartheta}(\vartheta_d, \delta_d)\ddot{\vartheta}_d + c_\vartheta(\vartheta_d, \delta_d, \dot{\vartheta}_d, \dot{\delta}_d) + g_\vartheta(\vartheta_d, \delta_d) \\ & - H_{\vartheta\delta}(\vartheta_d, \delta_d)H_{\delta\delta}^{-1}(\vartheta_d, \delta_d)\Big(H_{\vartheta\delta}^T(\vartheta_d, \delta_d)\ddot{\vartheta}_d + c_\delta(\vartheta_d, \delta_d, \dot{\vartheta}_d, \dot{\delta}_d) \\ & + g_\delta(\vartheta_d) + K\delta_d + D\dot{\delta}_d\Big) \end{aligned} \tag{6.119}$$

$$K_P(t) = \Big(H_{\vartheta\vartheta}(\vartheta_d, \delta_d) - H_{\vartheta\delta}(\vartheta_d, \delta_d)H_{\delta\delta}^{-1}(\vartheta_d, \delta_d)H_{\vartheta\delta}^T(\vartheta_d, \delta_d)\Big)K_P \quad (6.120)$$

$$K_D(t) = \Big(H_{\vartheta\vartheta}(\vartheta_d, \delta_d) - H_{\vartheta\delta}(\vartheta_d, \delta_d)H_{\delta\delta}^{-1}(\vartheta_d, \delta_d)H_{\vartheta\delta}^T(\vartheta_d, \delta_d)\Big)K_D. \quad (6.121)$$

The initial conditions for numerical integration of (6.117) are typically $\delta_0 = \dot{\delta}_0 = 0$ associated with an undeformed rest configuration for the arm; however, any set of initial values could be used since this dynamics is asymptotically stable, as previously demonstrated.

An even simpler implementation of (6.118) is

$$u = u_d(t) + K_P(\vartheta_d - \vartheta) + K_D(\dot{\vartheta}_d - \dot{\vartheta}), \quad (6.122)$$

with constant feedback matrices.

6.4.2 Two-time scale control

An alternative nonlinear approach to the problem of joint trajectory tracking can be devised using the different time scale between the flexible body dynamics and the rigid body dynamics. The equations of motion of the robot arm can be separated into the rigid and flexible parts by considering the inverse M of the inertia matrix H, which can be partitioned as —see also (6.101)—

$$H^{-1}(\vartheta, \delta) = M(\vartheta, \delta) = \begin{pmatrix} M_{\vartheta\vartheta}(\vartheta, \delta) & M_{\vartheta\delta}(\vartheta, \delta) \\ M_{\vartheta\delta}^T(\vartheta, \delta) & M_{\delta\delta}(\vartheta, \delta) \end{pmatrix}. \quad (6.123)$$

Then, the model (6.75) becomes

$$\begin{aligned} \ddot{\vartheta} = {} & M_{\vartheta\vartheta}(\vartheta, \delta)(u - c_\vartheta(\vartheta, \delta, \dot{\vartheta}, \dot{\delta}) - g_\vartheta(\vartheta, \delta)) \\ & - M_{\vartheta\delta}(\vartheta, \delta)(c_\delta(\vartheta, \delta, \dot{\vartheta}, \dot{\delta}) + g_\delta(\vartheta) + D\dot{\delta} + K\delta) \quad (6.124) \\ \ddot{\delta} = {} & M_{\vartheta\delta}^T(\vartheta, \delta)(u - c_\vartheta(\vartheta, \delta, \dot{\vartheta}, \dot{\delta}) - g_\vartheta(\vartheta, \delta)) \\ & - M_{\delta\delta}(\vartheta, \delta)(c_\delta(\vartheta, \delta, \dot{\vartheta}, \dot{\delta}) + g_\delta(\vartheta) + D\dot{\delta} + K\delta). \quad (6.125) \end{aligned}$$

Time scale separation is intuitively determined by the values of oscillation frequencies of flexible links and in turn by the magnitudes of the elements of K (see Section 6.1). In detail, consider the smallest stiffness coefficient K_m so that the diagonal matrix K can be factored as $K = K_m\bar{K}$. The *elastic force* variables can be defined as

$$z = K_m\bar{K}\delta = \frac{1}{\epsilon^2}\bar{K}\delta, \quad (6.126)$$

and accordingly the model (6.124) and (6.125) can be rewritten as

$$\ddot{\vartheta} = M_{\vartheta\vartheta}(\vartheta, \epsilon^2 z)\left(u - c_\vartheta(\vartheta, \epsilon^2 z, \dot{\vartheta}, \epsilon^2 \dot{z}) - g_\vartheta(\vartheta, \epsilon^2 z)\right)$$
$$- M_{\vartheta\delta}(\vartheta, \epsilon^2 z)\left(c_\delta(\vartheta, \epsilon^2 z, \dot{\vartheta}, \epsilon^2 \dot{z}) + g_\delta(\vartheta) + \epsilon^2 D\bar{K}^{-1}\dot{z} + z\right) \quad (6.127)$$
$$\epsilon^2 \ddot{z} = \bar{K} M_{\vartheta\delta}^T(\vartheta, \epsilon^2 z)\left(u - c_\vartheta(\vartheta, \epsilon^2 z, \dot{\vartheta}, \epsilon^2 \dot{z}) - g_\vartheta(\vartheta, \epsilon^2 z)\right)$$
$$- \bar{K} M_{\delta\delta}(\vartheta, \epsilon^2 z)\left(c_\delta(\vartheta, \epsilon^2 z, \dot{\vartheta}, \epsilon^2 \dot{z}) + g_\delta(\vartheta) + \epsilon^2 D\bar{K}^{-1}\dot{z} + z\right). \quad (6.128)$$

Eqs. (6.127) and (6.128) represent a *singularly perturbed* form of the flexible arm model, where ϵ is the so-called *perturbation parameter*. Although the model can be always recast as above, this form is significant only when ϵ is small, meaning that an effective time scale separation occurs; in particular, the flexural rigidity EI and the length ℓ of each link concur to determine the magnitude of the perturbation parameter and influence the validity of the approach.

When $\epsilon \to 0$, the model of an *equivalent* rigid arm is recovered. In fact, setting $\epsilon = 0$ and solving for z in (6.128) gives

$$z_s = M_{\delta\delta}^{-1}(\vartheta_s, 0) M_{\vartheta\delta}^T(\vartheta_s, 0)\left(u_s - c_\vartheta(\vartheta_s, 0, \dot{\vartheta}_s, 0) - g_\vartheta(\vartheta_s, 0)\right)$$
$$- c_\delta(\vartheta_s, 0, \dot{\vartheta}_s, 0) - g_\delta(\vartheta_s), \quad (6.129)$$

where subscript s indicates that the system is considered in the *slow* time scale. Plugging (6.129) into (6.127) with $\epsilon = 0$ yields

$$\ddot{\vartheta}_s = \left(M_{\vartheta\vartheta}(\vartheta_s, 0) - M_{\vartheta\delta}(\vartheta_s, 0) M_{\delta\delta}^{-1}(\vartheta_s, 0) M_{\vartheta\delta}^T(\vartheta_s, 0)\right) \cdot$$
$$\left(u_s - c_\vartheta(\vartheta_s, 0, \dot{\vartheta}_s, 0) - g_\vartheta(\vartheta_s, 0)\right). \quad (6.130)$$

It is not difficult to check that

$$M_{\vartheta\vartheta}(\vartheta_s, 0) - M_{\vartheta\delta}(\vartheta_s, 0) M_{\delta\delta}^{-1}(\vartheta_s, 0) M_{\vartheta\delta}^T(\vartheta_s, 0) = H_{\vartheta\vartheta}^{-1}(\vartheta_s, 0) \quad (6.131)$$

where $H_{\vartheta\vartheta}(\vartheta_s, 0)$ is the inertia matrix of the equivalent rigid arm, so that eq. (6.130) becomes

$$H_{\vartheta\vartheta}(\vartheta_s, 0)\ddot{\vartheta}_s + c_\vartheta(\vartheta_s, 0, \dot{\vartheta}_s, 0) + g_\vartheta(\vartheta_s, 0) = u_s. \quad (6.132)$$

In order to study the dynamics of the system in the *fast* time scale, the so-called *boundary-layer* subsystem has to be identified. This can be obtained by setting $\tau = t/\epsilon$, treating the slow variables as constants in the

fast time scale, and introducing the fast variables $z_f = z - z_s$; thus, the fast subsystem of (6.128) is

$$\frac{d^2 z_f}{d\tau^2} = -\bar{K} M_{\delta\delta}(\vartheta_s, 0) z_f + \bar{K} M^T_{\vartheta\delta}(\vartheta_s, 0) u_f, \tag{6.133}$$

where the fast control $u_f = u - u_s$ has been introduced accordingly.

On the basis of the above two-time scale model, the design of a feedback controller for the system (6.127) and (6.128) can be performed according to a *composite control* strategy, i.e.,

$$u = u_s(\vartheta_s, \dot{\vartheta}_s) + u_f(z_f, dz_f/d\tau) \tag{6.134}$$

with the constraint that $u_f(0,0) = 0$, so that u_f is inactive along the equilibrium manifold specified by (6.129).

The slow control for the rigid nonlinear subsystem (6.132) can be designed according to the well-known inverse dynamics concept used for rigid manipulators. On the other hand, the fast subsystem is a marginally stable linear slowly time-varying system that can be stabilized by a fast control, e.g., based on classical pole placement techniques; an output feedback design is typically required to face the lack of measurements for the derivatives of flexible variables.

By applying Tikhonov's theorem, it can be shown that under the composite control (6.134), the goal of tracking a desired joint trajectory together with stabilizing the deflections around the equilibrium manifold, naturally established by the rigid subsystem under the slow control, is achieved with an order of ϵ approximation. A robustness analysis relative to the magnitude of the perturbation parameter can be performed. When ϵ is not small enough, the use of integral manifolds to obtain a more accurate slow subsystem that accounts for the effects of flexibility up to a certain order of ϵ represents a viable strategy to make the composite control perform satisfactorily.

Finally, comparing (6.107) with the inversion control law based on (6.132) clearly points out the difference between the synthesis at the joint level using the full dynamics and the one restricted to the equivalent rigid arm model.

6.5 End-effector tracking control

The problem of accurate end-effector trajectory tracking is the most difficult one for flexible manipulators. Even when an effective control strategy has been designed at the joint level, still considerable vibration at the arm tip

may be observed during motion for a lightly damped structure. From an input–output point of view, we may try to use the n available joint torque inputs for controlling n output variables characterizing the tip position, i.e., for reproducing a desired trajectory $y_d(t)$. We remark that the choice of suitable reference trajectories that do not induce large deflections and excite arm vibrations in the frequency range of interest is more critical than in the joint tracking case.

In this respect, the direct extension of the inversion strategy to the end-effector output typically leads to closed-loop instabilities, nominally generating unbounded deformations and/or very large applied torques. In practice, joint actuators saturate and a jerky arm behaviour is observed, while control of tip motion is completely lost.

This phenomenon is present both in the linear (one-link) and nonlinear (multilink) cases. In fact, according to the modelling presented in Section 6.1, the transfer function of a one-link flexible arm contains stable zeros when the output position is co-located with the joint actuation, but will present pairs of real stable/unstable zeros when the output is relocated at the tip; this qualifies a *nonminimum phase* transfer function. Then, when the system is inverted, feedback *cancellation* of nonminimum phase zeros with unstable poles produces internal instability, not observable in the input–output map. Similarly, it can be shown that the *end-effector zero dynamics* of a multilink flexible arm, i.e., the unobservable dynamics associated with an input action which attempts to keep the end-effector output at a constant (zero) value, is *unstable*; by analogy to the linear case, this situation is referred to as nonminimum phase. Again, since inversion control is designed for cancelling this zero dynamics, closed-loop instability occurs.

Following the above discussion, we can infer that the trajectory tracking problem for nonminimum phase systems has to be handled either by resorting to a suitable feedforward strategy or by avoiding exact feedback cancellation. In both cases, it is convenient to define the desired arm behaviour not in terms of $(\vartheta_d(t), \delta_d(t))$ but equivalently in terms of $(y_d(t), \delta_d(t))$, where y is one-to-one related to the tip position. A bounded evolution $\delta_d(t)$ of the arm deformation variables will then be computed on the basis of the given output trajectory $y_d(t)$, as a natural motion of the system.

An open-loop solution, suitable for the *one-link linear case*, will be derived defining the inversion procedure in the *frequency domain* by assuming that the given trajectory $y_d(t)$ is part of a periodic signal. This solution leads to a *noncausal* command, since the obtained input $u_d(t)$ anticipates the actual start of the reference output trajectory. A more general technique will be presented that computes the bounded evolution $\delta_d(t)$ through the solution of a set of (nonlinear) partial differential equations depend-

ing on the desired output trajectory; a time-varying reference state is then constructed and used in a combined feedforward/feedback strategy, where the feedback part stabilizes the system around the state trajectory. Thus, *nonlinear regulation* will be achieved with simultaneous closed-loop stabilization and output trajectory tracking; the latter is in general obtained only asymptotically, depending on the initial conditions of the arm.

6.5.1 Frequency domain inversion

Consider a one-link flexible arm model in the generic form

$$\begin{pmatrix} h_{\vartheta\vartheta} & h_{\delta\vartheta}^T \\ h_{\delta\vartheta} & H_{\delta\delta} \end{pmatrix} \begin{pmatrix} \ddot{\vartheta}(t) \\ \ddot{\delta}(t) \end{pmatrix} + \begin{pmatrix} 0 & 0 \\ 0 & D \end{pmatrix} \begin{pmatrix} \dot{\vartheta}(t) \\ \dot{\delta}(t) \end{pmatrix} + \begin{pmatrix} 0 & 0 \\ 0 & K \end{pmatrix} \begin{pmatrix} \vartheta(t) \\ \delta(t) \end{pmatrix} = \begin{pmatrix} u(t) \\ 0 \end{pmatrix} \tag{6.135}$$

that can be any of the models derived in Section 6.1. The tip position output associated with (6.135) can be written as

$$y(t) = \begin{pmatrix} 1 & c_e^T \end{pmatrix} \begin{pmatrix} \vartheta(t) \\ \delta(t) \end{pmatrix}, \tag{6.136}$$

where $c_e = \varphi'(\ell)$ expresses the contributions of each mode shape to the tip angular position.

In order to reproduce a desired smooth time profile $y_d(t)$, a stable inversion of the system can be set up in the Fourier domain by regarding both the input and the output as periodic functions. In this way, provided that the involved signals are Fourier-transformable, all quantities will automatically be bounded over time. The intrinsic assumption of this method leads to the *open-loop* computation of an input command $u_d(t)$ that will be used as a feedforward on the real system.

We start by rewriting eq. (6.135) as

$$\begin{pmatrix} h_{\vartheta\vartheta} & h_{\delta\vartheta}^T - h_{\vartheta\vartheta} c_e^T \\ h_{\delta\vartheta} & H_{\delta\delta} - h_{\delta\vartheta} c_e^T \end{pmatrix} \begin{pmatrix} \ddot{y}(t) \\ \ddot{\delta}(t) \end{pmatrix} + \begin{pmatrix} 0 & 0 \\ 0 & D \end{pmatrix} \begin{pmatrix} \dot{y}(t) \\ \dot{\delta}(t) \end{pmatrix} + \begin{pmatrix} 0 & 0 \\ 0 & K \end{pmatrix} \begin{pmatrix} y(t) \\ \delta(t) \end{pmatrix} = \begin{pmatrix} u(t) \\ 0 \end{pmatrix}, \tag{6.137}$$

where (6.136) has been used. Let then

$$\ddot{Y}(\omega) = \int_{-\infty}^{\infty} \exp(-j\omega t) \ddot{y}(t) dt \tag{6.138}$$

be the bilateral Fourier transform of the output acceleration; hence, eq.

(6.137) can be rewritten in the frequency domain as

$$\begin{pmatrix} h_{\vartheta\vartheta} & h_{\delta\vartheta}^T - h_{\vartheta\vartheta} c_e^T \\ h_{\delta\vartheta} & H_{\delta\delta} - h_{\delta\vartheta} c_e^T + \dfrac{1}{j\omega} D - \dfrac{1}{\omega^2} K \end{pmatrix} \begin{pmatrix} \ddot{Y}(\omega) \\ \ddot{\Delta}(\omega) \end{pmatrix} = \begin{pmatrix} U(\omega) \\ 0 \end{pmatrix}, \quad (6.139)$$

where $\ddot{\Delta}(\omega)$ and $U(\omega)$ are the Fourier transforms of the flexible accelerations and of the input torque, respectively. Inverting eq. (6.139) gives

$$\begin{pmatrix} \ddot{Y}(\omega) \\ \ddot{\Delta}(\omega) \end{pmatrix} = \begin{pmatrix} g_{11}(\omega) & g_{12}^T(\omega) \\ g_{21}(\omega) & G_{22}(\omega) \end{pmatrix} \begin{pmatrix} U(\omega) \\ 0 \end{pmatrix}, \quad (6.140)$$

and thus

$$U(\omega) = \frac{1}{g_{11}(\omega)} \ddot{Y}(\omega) = r(\omega) \ddot{Y}(\omega). \quad (6.141)$$

When a desired symmetric zero-mean acceleration profile $\ddot{y}_d(t)$ is given such that $\ddot{y}_d(t) = 0$ for $t \leq -T/2$ and $t \geq T/2$, this signal can be embedded in a periodic one and the Fourier transform (6.138) can be truncated outside the interval $[-T/2, T/2]$. Plugging $\ddot{Y}_d(\omega)$ in (6.141) yields $U_d(\omega)$, which generates the required input torque $u_d(t)$ through finite inverse Fourier transformation.

The obtained time profile expands beyond the interval $[-T/2, T/2]$, since the inverse system is *noncausal*. In fact, the command $u_d(t)$ can be also expressed as

$$u_d(t) = \int_{-\infty}^{\infty} r(t-\tau) \ddot{y}_d(\tau) d\tau = \int_{-T/2}^{T/2} r(t-\tau) \ddot{y}_d(\tau) d\tau, \quad (6.142)$$

where $r(t)$ is the impulsive time response of the inverse system corresponding to $r(\omega)$ in (6.141); since here $r(t-\tau) \neq 0$ also for $t < \tau$, then $u_d(t) \neq 0$ also for $t < -T/2$. In practice, the energy content of the required input torque will rapidly decay to zero outside the desired interval duration T of the output motion, and a time truncation can be reasonably performed.

It should be noted that eq. (6.140) provides also the frequency-based description of the flexible variables associated with the given output motion, which can be converted as well into a time evolution $\delta_d(t)$. In particular, the initial values $\delta_d(-T/2)$ and $\dot{\delta}_d(-T/2)$ correspond to the specific initial arm deflection state which gives overall bounded deformation under inversion control.

Finally, we remark that a noncausal behaviour of the inverse system is obtained whenever the original system presents a finite time delay between the input action and the observed output effects.

The above technique is inherently based on linear concepts, and the extension to the nonlinear multilink case can be performed only by iterating its application to repeated linear approximations of the system along the nominal trajectory.

6.5.2 Nonlinear regulation

The problem of achieving output tracking, at least asymptotically, while enforcing internal state stability is a classical *regulation problem*, whose solution is widely known in the linear case under full state feedback. The extension of the same approach to the nonlinear setting requires some technical assumptions and involves a larger amount of off-line computation, but it is rather straightforward in the robotic case.

The key point is to compute a *bounded* reference state trajectory for the flexible arm so as to produce the desired output motion. In connection with any bounded and smooth output trajectory $y_d(t)$, typically generated by an autonomous dynamic system (an *exosystem*), such a trajectory $(\vartheta_d(t), \delta_d(t))$ surely exists. The control law can then be chosen as formed by two contributions; namely, a *feedforward* term which drives the system trajectories along their desired evolution, and a *state feedback* term necessary to stabilize the closed-loop dynamics around the nominal trajectory. This stabilizing action can be typically designed using only first-order information, i.e., as a linear feedback, in view of the local controllability of the manipulator equations. Once the flexible arm is in the proper deformation state, only the feedforward term is active.

For convenience, we consider a generalization of (6.136) as system output, i.e.,

$$y = \vartheta + C\delta, \tag{6.143}$$

where the elements in the constant matrix C include the contributions of link mode shapes. On the assumption of small deformation, this output is one-to-one related to the Cartesian position and orientation of the tip through the standard direct kinematics of the arm.

Moreover, we assume that the output reference trajectory is generated by an exosystem that can be chosen, without loss of generality, as a linear system in observable canonical form with

$$Y_d = \{y_{di}, \dot{y}_{di}, \ddot{y}_{di}, \ldots, y_{di}^{r_i-1};\ i = 1, \ldots, n\} \tag{6.144}$$

taken as its state; here, r_i is the smoothness degree of the i-th output trajectory.

The design of a nonlinear regulator is simplified by rewriting the manipulator dynamics (6.75) in terms of the new coordinates (y, δ) as

$$\begin{aligned} H_{\vartheta\vartheta}(y - C\delta, \delta)\ddot{y} + \big(H_{\vartheta\delta}(y - C\delta, \delta) - H_{\vartheta\vartheta}(y - C\delta, \delta)C\big)\ddot{\delta} \\ + c_{\vartheta}(y - C\delta, \delta, \dot{y} - C\dot{\delta}, \dot{\delta}) + g_{\vartheta}(y - C\delta, \delta) = u \end{aligned} \tag{6.145}$$

$$\begin{aligned} H^T_{\vartheta\delta}(y - C\delta, \delta)\ddot{y} + \big(H_{\delta\delta}(y - C\delta, \delta) - H^T_{\vartheta\delta}(y - C\delta, \delta)C\big)\ddot{\delta} \\ + c_{\delta}(y - C\delta, \delta, \dot{y} - C\dot{\delta}, \dot{\delta}) + g_{\delta}(y - C\delta) + D\dot{\delta} + K\delta = 0, \end{aligned} \tag{6.146}$$

where (6.143) has been used.

In order to determine the reference state evolution associated with $y_d(t)$, it is sufficient to specify only $\delta_d(t)$ and its derivative $\dot{\delta}_d(t)$. Hence, the problem reduces to determining the vector functions $\delta_d = \pi(Y_d)$ and $\dot{\delta}_d = (\partial\pi/\partial Y_d)\dot{Y}_d$. In particular, the function $\pi(Y_d)$ should satisfy eq. (6.146), evaluated along the reference evolution of the output, i.e.,

$$\begin{aligned} H^T_{\vartheta\delta}(y_d, \pi(Y_d))\ddot{y}_d + \big(H_{\delta\delta}(y_d, \pi(Y_d)) - H^T_{\vartheta\delta}(y_d, \pi(Y_d))C\big)\ddot{\pi}(Y_d, \dot{Y}_d, \ddot{Y}_d) \\ + c_{\delta}(y_d, \pi(Y_d), \dot{y}_d, \dot{\pi}(Y_d, \dot{Y}_d)) + g_{\delta}(y_d, \pi(Y_d)) \\ + D\dot{\pi}(Y_d, \dot{Y}_d) + K\pi(Y_d) = 0. \end{aligned} \tag{6.147}$$

This equation is independent of the applied torque and should be considered as a dynamic constraint for $\pi(Y_d)$. Being (6.147) a *nonlinear time-varying* differential equation, it is usually impossible to determine a bounded solution in closed form. We notice that this equation reduces to a matrix format in the case of linear systems, as for the one-link flexible arm.

A feasible approach is to build an approximate solution $\hat{\pi}(Y_d)$ for the arm deformation by using basis elements which are bounded functions of their arguments, e.g., polynomials in Y_d. As long as each component $y_{di}(t)$ of the desired trajectory and its derivatives up to order (r_i+1) are bounded, the approximation $\hat{\pi}(Y_d)$ is necessarily a bounded function of time. The problem of determining the constant coefficients in the expansion can then be solved through a recursive procedure using the polynomial identity principle.

Once a solution $\hat{\pi}(Y_d) \approx \pi(Y_d)$ is obtained up to any desired accuracy, back-substitution of the reference deformation δ_d, of the desired output trajectory y_d, and of their time derivatives into (6.145) will give the nominal feedforward regulation term as

$$\begin{aligned} u_d &= H_{\vartheta\vartheta}(y_d, \delta_d)\ddot{y}_d + (H_{\vartheta\delta}(y_d, \delta_d) - H_{\vartheta\vartheta}(y_d, \delta_d)C)\,\ddot{\delta}_d \\ &\quad + c_{\vartheta}(y_d, \delta_d, \dot{y}_d, \dot{\delta}_d) + g_{\vartheta}(y_d, \delta_d) \\ &= \gamma(Y_d, \dot{Y}_d, \ddot{Y}_d). \end{aligned} \tag{6.148}$$

The nonlinear regulator law takes on the final form

$$u = u_d + \hat{F} \begin{pmatrix} y_d - y \\ \dot{y}_d - \dot{y} \\ \delta_d - \delta \\ \dot{\delta}_d - \dot{\delta} \end{pmatrix} = u_d + F \begin{pmatrix} \vartheta_d - \vartheta \\ \dot{\vartheta}_d - \dot{\vartheta} \\ \delta_d - \delta \\ \dot{\delta}_d - \dot{\delta} \end{pmatrix}, \qquad (6.149)$$

where the feedback matrix F stabilizes the linear approximation of the system dynamics. Indeed, if a global stabilizer is available, convergence to the reference state behaviour can be achieved from *any* initial state. In particular, a PD feedback on the joint variables ϑ alone was shown to stabilize any arm configuration; as a result, a simplified form of F can be used in (6.149), and the overall regulator can be implemented using only *partial state* feedback.

It is worth noticing that solving eq. (6.147) for $\delta_d = \pi(Y_d)$ provides as a byproduct the unique initial state at time $t = 0$ that is bounded over the whole desired output motion. This should be related to the approach of the previous subsection.

While the stability property of the regulator approach rules out inversion techniques for end-effector tracking, it should be stressed that only *asymptotic* output reproduction can be guaranteed if the initial state of the flexible arm does not coincide with the solution to (6.147) at time $t = 0$. Moreover, during error transients, the input–output behaviour of the closed-loop system is still described by a fully nonlinear dynamics, contrary to the inversion case.

6.6 Further reading

A recent tutorial on modelling, design, and control of flexible manipulator arms is available in [9].

Modal analysis based on Euler-Bernoulli beam equations can be found in classical mechanics textbooks, covering flexible-body dynamics, e.g., [36]. The issue of unconstrained vs. constrained mode expansion was discussed in [3] and further in [7]. The dependence of the fundamental frequency of a single link on its shape and structure has been studied in [56]. The combined Lagrangian-assumed modes method for modelling multilink flexible arms is due to [8]; discussion on infinite-dimensional models can be found in [25], and the effect of mode truncation was studied in [31]. Alternative approaches to the assumed modes method are the finite-element approach [52] and the Ritz-Kantorovich expansions [53]. The use of symbolic software packages for dynamic modelling of manipulators with both joint and link flexibility was proposed in [11]. Early work on modelling,

identification and control of a single-link flexible arm was carried out in, e.g., [10, 45, 27, 57, 58]. Analysis of the finite- and infinite-dimensional transfer functions was performed in [29, 55]. Two-link flexible arms were studied in, e.g., [37, 38].

Performance of co-located joint feedback controllers was investigated in [12]. The importance of dynamic models for control of flexible manipulators was pointed out in [22], and a symbolic closed-form model was derived in [21]. The problem of joint regulation of flexible arms under gravity was solved in [23] where also the case of no damping is covered; the control scheme was extended to tip regulation in [46]. An iterative learning scheme for positioning the end effector without knowledge of the gravity term is given in [19]. For enhancement of structural passive damping, the reader is referred to [1]. Active vibration linear control was proposed by [50, 51] and further refined by [14]. Inversion-based controllers that achieve input–output linearization were derived in [24]; the use of the feedforward strategy was tested in [15]. Two-time scale control was proposed by [47] and extended to the output feedback setting in [49]; a refinement of the singularly perturbed model via the use of integral manifolds can be found in [48]. A combined feedback linearization/singular perturbation approach was recently presented in [54]. An overview on the use of perturbation techniques in control of flexible manipulators is given in [26]. Robust schemes using H_∞ control for a one-link flexible arm were proposed in [42, 2]. Alternative techniques for stabilization and trajectory tracking were proposed in [33] using direct strain feedback, and in [30] using acceleration feedback. A state observer for a two-link flexible arm has been designed and implemented in [39].

The problem of suitable trajectory generation for flexible arms was investigated in [5, 28]. The frequency domain approach was presented in [4] for the single-link flexible arm, and was extended to the multilink case in [6]. Performance of non-colocated tip feedback controllers was investigated in [13]. The use of inversion control for stable tracking of an output chosen along the links was proposed in [18], and a control scheme for a single-link flexible arm was proposed in [20]. The problem of output regulation of a flexible robot arm was studied in [16] and a comparison of approaches based on regulation theory is given in [17]. Related work on the use of a partial state feedback regulator can be found in [40]. Stable tip trajectory control for multilink flexible arms is studied in the time domain in [32, 59].

Only planar deformation of flexible arms has been considered in this chapter. A challenging problem is the control of both bending and torsional vibrations for multilink flexible arms; satisfactory results for a single-link arm can be found in [44, 34]. A new line of research concerns the problem

of position and force control of flexible link manipulators; preliminary work is reported in [43, 35].

References

[1] T.E. Alberts, L.J. Love, E. Bayo, and H. Moulin, "Experiments with end-point control of a flexible link using the inverse dynamics approach and passive damping," *Proc. 1990 American Control Conf.*, San Diego, CA, pp. 350–355, 1990.

[2] R.N. Banavar and P. Dominic, "An LQG/H_∞ controller for a flexible manipulator," *IEEE Trans. on Control Systems Technology*, vol. 3, pp. 409–416, 1995.

[3] E. Barbieri and Ü. Özgüner, "Unconstrained and constrained mode expansions for a flexible slewing link," *ASME J. of Dynamic Systems, Measurement, and Control*, vol. 110, pp. 416–421, 1988.

[4] E. Bayo, "A finite-element approach to control the end-point motion of a single-link flexible robot," *J. of Robotic Systems*, vol. 4, pp. 63–75, 1987.

[5] E. Bayo and B. Paden, "On trajectory generation for flexible robots," *J. of Robotic Systems*, vol. 4, pp. 229–235, 1987.

[6] E. Bayo, M.A. Serna, P. Papadopoulus, and J. Stubbe, "Inverse dynamics and kinematics of multi-link elastic robots: An iterative frequency domain approach," *Int. J. of Robotics Research*, vol. 8, no. 6, pp. 49–62, 1989.

[7] F. Bellezza, L. Lanari, and G. Ulivi, "Exact modeling of the slewing flexible link," *Proc. 1990 IEEE Int. Conf. on Robotics and Automation*, Cincinnati, OH, pp. 734–739, May 1990.

[8] W.J. Book, "Recursive Lagrangian dynamics of flexible manipulator arms," *Int. J. of Robotics Research*, vol. 3, no. 3, pp. 87–101, 1984.

[9] W.J. Book, "Controlled motion in an elastic world," *ASME J. of Dynamic Systems, Measurement, and Control*, vol. 115, pp. 252–261, 1993.

[10] R.H. Cannon and E. Schmitz, "Initial experiments on the end-point control of a flexible one-link robot," *Int. J. of Robotics Research*, vol. 3, no. 3, pp. 62–75, 1984.

[11] S. Cetinkunt and W.J. Book, "Symbolic modeling and dynamic simulation of robotic manipulators with compliant links and joints," *Robotics & Computer-Integrated Manufacturing*, vol. 5, pp. 301–310, 1989.

[12] S. Cetinkunt and W.J. Book, "Performance limitations of joint variable-feedback controllers due to manipulator structural flexibility," *IEEE Trans. on Robotics and Automation*, vol. 6, pp. 219–231, 1990.

[13] S. Cetinkunt and W.L. Yu, "Closed-loop behavior of a feedback controlled flexible arm: A comparative study," *Int. J. of Robotics Research*, vol. 10, pp. 263-275, 1991.

[14] A. Das and S.N. Singh, "Dual mode control of an elastic robotic arm: Nonlinear inversion and stabilization by pole assignment," *Int. J. of Systems Science*, vol. 21, pp. 1185–1204, 1990.

[15] A. De Luca, L. Lanari, P. Lucibello, S. Panzieri, and G. Ulivi, "Control experiments on a two-link robot with a flexible forearm," *Proc. 29th IEEE Conf. on Decision and Control*, Honolulu, HI, pp. 520–527, 1990.

[16] A. De Luca, L. Lanari, and G. Ulivi, "Output regulation of a flexible robot arm," in *Analysis and Optimization of Systems*, A. Bensoussan and J.L. Lions (Eds.), Lecture Notes in Control and Information Sciences, Springer-Verlag, Berlin, D, vol. 144, pp. 833–842, 1990.

[17] A. De Luca, L. Lanari, and G. Ulivi, "End-effector trajectory tracking in flexible arms: Comparison of approaches based on regulation theory," in *Advanced Robot Control — Proc. Int. Workshop on Nonlinear and Adaptive Control: Issues in Robotics*, C. Canudas de Wit (Ed.), Lecture Notes in Control and Information Sciences, Springer-Verlag, Berlin, D, vol. 162, pp. 190–206, 1991.

[18] A. De Luca, P. Lucibello, and G. Ulivi, "Inversion techniques for trajectory control of flexible robot arms," *J. of Robotic Systems*, vol. 6, pp. 325–344, 1989.

[19] A. De Luca and S. Panzieri, "End-effector regulation of robots with elastic elements by an iterative scheme," *Int. J. of Adaptive Control and Signal Processing*, vol. 10, pp. 379–393, 1996.

[20] A. De Luca and B. Siciliano, "Trajectory control of a non-linear one-link flexible arm," *Int. J. of Control*, vol. 50, pp. 1699–1716, 1989.

[21] A. De Luca and B. Siciliano, "Closed-form dynamic model of planar multilink lightweight robots," *IEEE Trans. on Systems, Man, and Cybernetics*, vol. 21, pp. 826–839, 1991.

[22] A. De Luca and B. Siciliano, "Relevance of dynamic models in analysis and synthesis of control laws for flexible manipulators," in *Robotics and Flexible Manufacturing Systems*, S.G. Tsafestas and J.C. Gentina (Eds.), Elsevier, Amsterdam, NL, pp. 161–168, 1992.

[23] A. De Luca and B. Siciliano, "Regulation of flexible arms under gravity," *IEEE Trans. on Robotics and Automation*, vol. 9, pp. 463–467, 1993.

[24] A. De Luca and B. Siciliano, "Inversion-based nonlinear control of robot arms with flexible links," *AIAA J. of Guidance, Control, and Dynamics*, vol. 16, pp. 1169–1176, 1993.

[25] X. Ding, T.J. Tarn, and A.K. Bejczy, "A novel approach to the modelling and control of flexible robot arms," *Proc. 27th IEEE Conf. on Decision and Control*, Austin, TX, pp. 52–57, 1988.

[26] A.R. Fraser and R.W. Daniel, *Perturbation Techniques for Flexible Manipulators*, Kluwer Academic Publishers, Boston, MA, 1991.

[27] G.G. Hastings and W.J. Book, "A linear dynamic model for flexible robotic manipulators," *IEEE Control Systems Mag.*, vol. 7, no. 1, pp. 61–64, 1987.

[28] J.M. Hyde and W.P. Seering, "Using input command pre-shaping to suppress multiple mode vibration," *Proc. 1991 IEEE Int. Conf. on Robotics and Automation*, Sacramento, CA, pp. 2604–2609, 1991.

[29] H. Kanoh, "Distributed parameter models of flexible robot arms," *Advanced Robotics*, vol. 5, pp. 87–99, 1991.

[30] F. Khorrami and S. Jain, "Nonlinear control with end-point acceleration feedback for a two-link flexible manipulator: Experimental results," *J. of Robotic Systems*, vol. 10, pp. 505–530, 1993.

[31] J. Lin and F.L. Lewis, "Enhanced measurement and estimation methodology for flexible arm control," *J. of Robotic Systems*, vol. 11, pp. 367–385, 1994.

[32] P. Lucibello and M.D. Di Benedetto, "Output tracking for a nonlinear flexible arm," *ASME J. of Dynamic Systems, Measurement, and Control*, vol. 115, pp. 78–85, 1993.

[33] Z.-H. Luo, "Direct strain feedback control of flexible robot arms: New theoretical and experimental results," *IEEE Trans. on Automatic Control*, vol. 38, pp. 1610–1622, 1993.

[34] F. Matsuno, T. Murachi, and Y. Sakawa, "Feedback control of decoupled bending and torsional vibrations of flexible beams," *J. of Robotic Systems*, vol. 11, pp. 341–353, 1994.

[35] F. Matsuno and K. Yamamoto, "Dynamic hybrid position/force control of a two degree-of-freedom flexible manipulator," *J. of Robotic Systems*, vol. 11, pp. 355–366, 1994.

[36] L. Meirovitch, *Analytical Methods in Vibrations*, Macmillan, New York, NY, 1967.

[37] C.M. Oakley and R.H. Cannon, "Initial experiments on the control of a two-link manipulator with a very flexible forearm," *Proc. 1988 American Control Conf.*, Atlanta, GA, pp. 996–1002, 1988.

[38] C.M. Oakley and R.H. Cannon, "Equations of motion for an experimental planar two-link flexible manipulator," *Proc. 1989 ASME Winter Annual Meet.*, San Francisco, CA, pp. 267–278, 1989.

[39] S. Panzieri and G. Ulivi, "Design and implementation of a state observer for a flexible robot," *Proc. 1993 IEEE Int. Conf. on Robotics and Automation*, Atlanta, GA, vol. 3, pp. 204–209, 1993.

[40] F. Pfeiffer, "A feedforward decoupling concept for the control of elastic robots," *J. of Robotic Systems*, vol. 6, pp. 407–416, 1989.

[41] H.R. Pota and T.E. Alberts, "Multivariable transfer functions for a slewing piezoelectric laminate beam," *ASME J. of Dynamic Systems, Measurement, and Control*, vol. 117, pp. 352–359, 1995.

[42] T. Ravichandran, G. Pang, and D. Wang, "Robust H_∞ control of a single flexible link," *Control — Theory and Advanced Technology*, vol. 9, pp. 887–908, 1993.

[43] K. Richter and F. Pfeiffer, "A flexible link manipulator as a force measuring and controlling unit," *Proc. 1991 IEEE Int. Conf. on Robotics and Automation*, Sacramento, CA, pp. 1214–1219, 1991.

[44] Y. Sakawa and Z.H. Luo, "Modeling and control of coupled bending and torsional vibrations of flexible beams," *IEEE Trans. on Automatic Control*, vol. 34, pp. 970–977, 1989.

[45] Y. Sakawa, F. Matsuno, and S. Fukushima, "Modelling and feedback control of a flexible arm," *J. of Robotic Systems*, vol. 2, pp. 453–472, 1985.

[46] B. Siciliano, "An inverse kinematics scheme for flexible manipulators," *Proc. 2nd IEEE Mediterranean Symp. on New Directions in Control & Automation*, Chania, GR, pp. 543–548, 1994.

[47] B. Siciliano and W.J. Book, "A singular perturbation approach to control of lightweight flexible manipulators," *Int. J. of Robotics Research*, vol. 7, no. 4, pp. 79–90, 1988.

[48] B. Siciliano, W.J. Book, and G. De Maria, "An integral manifold approach to control of a one link flexible arm," *Proc. 25th IEEE Conf. on Decision and Control*, Athina, GR, pp. 1131–1134, 1986.

[49] B. Siciliano, J.V.R. Prasad, and A.J. Calise, "Output feedback two-time scale control of multi-link flexible arms," *ASME J. of Dynamic Systems, Measurement, and Control*, vol. 114, pp. 70–77, 1992.

[50] S.N. Singh and A.A. Schy, "Control of elastic robotic systems by nonlinear inversion and modal damping," *ASME J. of Dynamic Systems, Measurement, and Control*, vol. 108, pp. 180–189, 1986.

[51] S.N. Singh and A.A. Schy, "Elastic robot control: Nonlinear inversion and linear stabilization," *IEEE Trans. on Aerospace and Electronic Systems*, vol. 22, pp. 340–348, 1986.

[52] W.H. Sunada and S. Dubowsky, "The application of finite element methods to the dynamic analysis of flexible linkage systems," *ASME J. of Mechanical Design*, vol. 103, pp. 643–651, 1983.

[53] P. Tomei and A. Tornambè, "Approximate modeling of robots having elastic links," *IEEE Trans. on Systems, Man, and Cybernetics*, vol. 18, pp. 831–840, 1988.

[54] M.W. Vandegrift, F.L. Lewis, and S.Q. Zhu, "Flexible-link robot arm control by a feedback linearization/singular perturbation approach," *J. of Robotic Systems*, vol. 11, pp. 591–603, 1994.

[55] D. Wang and M. Vidyasagar, "Transfer functions for a single flexible link," *Int. J. of Robotics Research*, vol. 10, pp. 540–549, 1991.

[56] F.-Y. Wang, "On the extremal fundamental frequencies of one-link flexible manipulators," *Int. J. of Robotics Research*, vol. 13, pp. 162–170, 1994.

[57] B.-S. Yuan, W.J. Book, and B. Siciliano, "Direct adaptive control of a one-link flexible arm with tracking," *J. of Robotic Systems*, vol. 6, pp. 663–680, 1989.

[58] S. Yurkovich, F.E. Pacheco, and A.P. Tzes, "On-line frequency domain identification for control of a flexible-link robot with varying payload," *IEEE Trans. on Automatic Control*, vol. 34, pp. 1300–1304, 1989.

[59] H. Zhao and D. Chen, "Exact and stable tip trajectory tracking for multi-link flexible manipulator," *Proc. 32nd IEEE Conf. on Decision and Control*, San Antonio, TX, pp. 1371–1376, 1993.